ENHANCEMENT TO HITRAN TO SUPPORT

THE NASA EOS PROGRAM

Contract NAS5-96023

Annual Progress Report No. 2

For the period April 21, 1997 through April 20, 1998

Principal Investigator
Kate P. Kirby

Co-Principal Investigator
Laurence S. Rothman

November 1998

Prepared for
National Aeronautics and Space Administration
Greenbelt, Maryland 20771

Smithsonian Institution
Astrophysical Observatory
Cambridge, Massachusetts 02138

The Smithsonian Astrophysical Observatory
is a member of the
Harvard-Smithsonian Center for Astrophysics

The NASA Technical Officer for this grant is Dr. Michael King,
Code 900, Goddard Space Flight Center, Greenbelt, Maryland 20771.

NAS5-96023

Enhancement to HITRAN to Support the NASA EOS Program

Annual Progress Report
April 1997 to April 1998

Dr. Laurence S. Rothman
Harvard-Smithsonian Center for Astrophysics
Atomic and Molecular Physics Division
Mail Stop 50, 60 Garden Street
Cambridge MA 02138

Abstract— The HITRAN molecular database has been enhanced with the object of providing improved capabilities for the **EOS** program scientists. HITRAN itself is the database of high-resolution line parameters of gaseous species expected to be observed by the **EOS** program in its remote sensing activities. The database is part of a larger compilation that includes IR cross-sections, aerosol indices of refraction, and software for filtering and plotting portions of the database. These properties have also been improved. The software has been advanced in order to work on multiple platforms. Besides the delivery of the compilation on CD-ROM, the effort has been directed toward making timely access of data and software on the world wide web.

keywords: Absorption, Atmosphere, Emission, HITRAN, IR Cross-sections, Radiance, Remote Sensing, Spectroscopy

1. Introduction

The purpose of this project is to develop and enhance the HITRAN molecular spectroscopic database and associated software to support the observational programs of the Earth Observing System (**EOS**). In particular, the focus is on the EOS projects: the Atmospheric Infrared Sounder (**AIRS**), the High-Resolution Dynamics Limb Sounder (**HIRDLS**), Measurements of Pollution in the Troposphere (**MOPITT**), the Tropospheric Emission Spectrometer (**TES**), and the Stratospheric Aerosol and Gas Experiment (**SAGE** III). The data requirements of these programs in terms of spectroscopy are varied, but usually call for additional spectral parameters or improvements to existing molecular bands. In addition, cross-section data for heavier molecular species must be expanded and made amenable to modeling in remote sensing. The effort in the current project also includes developing software and distribution to make access, manipulation, and use of HITRAN functional to the EOS program.

2. HITRAN Data Improvement

The effort to improve, enhance, and extend the HITRAN database continued at several levels. For the line-by-line portion of the compilation, the EOS observational requirements may be for completely updated spectroscopic parameters, including line positions, intensities, halfwidths, and temperature dependence coefficients. Often improving a subset of the parameters that are deficient may be sufficient at this time, such as the air-broadened halfwidth if that is causing a problem for adequate modeling. From discussions with the teams of the EOS experiments, one also wants to anticipate future requirements so that a heads-up approach is taken. This often takes the form of adding new bands for existing molecules (overtones and combination bands), adding new molecular absorbers that are trace constituents of the atmosphere, and completing spectroscopic parameters for the transitions (such as pressure-shift, etc.). Another major thrust of the data improvement of the compilation is the incorporation of absorption cross-sections. Unlike the line-by-line traditional HITRAN parameters, these data are used primarily for molecules with extremely dense spectra, such as the chlorofluorocarbons and "heavy" oxides of nitrogen. With recent advances in atmospheric modeling using the HITRAN format of cross-sections, the EOS community has benefitted from this approach.

2.1. Water vapor, H_2O

Spectroscopic parameters for water vapor and its principal isotopomers, $H_2{}^{18}O$, $H_2{}^{17}O$, and HDO, remain one of the top priorities for the HITRAN program. The deficiencies that remain with respect to the water vapor parameters have implications both in the long- and short-wavelength regions

A very serious issue relates to flux anomalies when calculating the earth's radiation budget in the near infrared. Much of the data in the near-IR in HITRAN dates from the first edition. Some of these data were obtained from grating spectrometer data, recorded on paper charts at a high-altitude observatory. We embarked on a program to both obtain new measurements in this region and to survey other observations that have recently been undertaken. The new data have almost all been performed under laboratory controlled conditions using high-resolution Fourier transform spectrometers. We engaged W.J. Phillips at Arnold AFB to take high-resolution spectra of self-broadened water vapor in the 1.5- and 1.9-μm regions. These spectra are being analyzed by R.L. Hawkins of AFRL, and will represent the first update of many of the line positions and intensities in these regions since the first edition of HITRAN (line positions, intensities, and halfwidths prior to the 1987 database are designated with the reference index zero). In this region, other groups have also been active. A joint effort between Ohio State University (K. Keppler) and the University of Giessen, Germany (M. Winnewisser) has been ongoing for some time. In addition to collaborating with this team, we are assessing the data being taken by groups in France (J.M. Flaud et al). The involvement of the latter group is essential in final validation and checking, especially of the quantum assignments and energy levels.

R.A. Toth (Jet Propulsion Laboratory) has recently completed an analysis of laboratory spectra of water vapor, isotopes, and hot bands for the 500-2580 cm^{-1} regions. Updates are in preparation for positions, intensities, air-broadening coefficients, self-broadening coefficients, and pressure-induced shifts. We are also working with L. Coudert of the University of Paris for improvements in the ν_2 region (see for example, L.H. Coudert, "Analysis of the line positions and line intensities in the ν_2 band of the water molecule," *J.Mol.Spectrosc* **181**, 246-273 (1997)).

Linda Brown of JPL has undertaken work on water vapor in support of **SAGE III** in the region 857 to 1040 NM. She is a coauthor of the HITRAN compilation and we expect that there will

be substantial improvement to HITRAN because of this effort.

It has also been noticed that the current compilation does not include the improved HDO positions and intensities reported in the literature (J.-M. Flaud, C. Camy-Peyret, A. Mahmoudi, and G. Guelachvili, "The ν_2 band of $HD^{16}O$," *Internat. J. Infrared and Millimeter Waves* **7,** 1063-1090 (1986); R.A. Toth, "$HD^{16}O$, $HD^{18}O$, and $HD^{17}O$ Transition Frequencies and Strengths in the ν_2 Bands," *J.Mol.Spectrosc.* **162,** 20-40 (1993)). We are in the process of acquiring these data for HITRAN from the principal authors. Some work will remain to cast these data into HITRAN form.

Line positions were updated for H_2O lines in the 720- to 1400-cm^{-1} region based on high-temperature measurements carried out at the Geophysics Directorate, Hanscom AFB. However, many bands still lack consistent self-broadened coefficients as well as pressure-shift coefficients.

A program to assess the differences between the available high-temperature water-vapor parameters has been undertaken. The databases include: (1) our HITEMP database which is based on the Direct Numerical Diagonalization (DND) technique (R.B. Wattson and L.S. Rothman, "Direct Numerical Diagonalization: Wave of the Future," *JQSRT* **48**, 763-780 (1992)); (2) the calculations of Jon Tennyson's group at the University of London (using a method analogous to ours); and (3) the ab initio calculations by David Schwenke of the NASA Ames Research Center. The effort to make the comparisons has been hampered by different formats, server crashes, unspecified units, and extremely large file sizes. In addition, each database has suffered from occasional incorrect line assignments. This situation requires attention, not only for the maintenance and evolution of the database, but for applying separate files of halfwidths and other quantum-dependent parameters.

2.2. Carbon dioxide, CO_2

The method of generating self-consistent spectroscopic parameters for both the HITRAN and HITEMP databases is described in the article by L.S. Rothman, R.L. Hawkins, R.B. Wattson, and R.R. Gamache, "Energy Levels, Intensities, and Linewidths of Atmospheric Carbon Dioxide Bands," *JQSRT* **48,** 537-566 (1992). High-resolution line position measurements of carbon dioxide are acquired from throughout the world and a least-squares method is used to generate consistent energy levels and positions. Likewise, intensities for the many bands considered for atmospheric and high-temperature applications are acquired. The DND method completes the database by calculating the

many bands that are unobtainable from the lab or field measurements.

The main area of improvement that we have been working on for carbon dioxide is in the short wavelength region. The group at NASA Ames (L. Giver and C. Chackerian) has been providing new data that is beginning to resolve the issues of incorrect Herman-Wallis factors and poor intensities due to perturbations that have existed for some of the bands in HITRAN. We have implemented some of their results, and will be adding more as they become available. Likewise in the shortwave region, the group at the College of William and Mary (V.M. Devi and D.C. Benner) collaborating with NASA Langley (C.P. Rinsland and M.A.H. Smith) will be providing data at 3 μm for the isotopomers, and for new broadening and shift coefficients.

A breakthrough has finally been achieved with respect to coming up with an acceptable scheme for representing the line coupling of CO_2. Ken Jucks of SAO in collaboration with J.M. Hartmann of the University of Paris, France have developed a parametrization that satisfies several requirements of the HITRAN database. It reduces the amount of data to be stored; updates and changes resulting from a modification of related database parameters (such as the air-broadened halfwidth) are easy to make; it requires a minimum of computer code changes for the modelers to utilize; it minimizes the risks and consequences of misuse. To achieve the latter, the sum rule is satisfied. An earlier attempt at parametrizing line coupling for carbon dioxide failed because this rule was not maintained at all temperatures considered in atmospheric radiance calculations. Another admirable feature of the method is that its formalism applies to other absorbers, such as methane and nitrous oxide.

2.3. Ozone, O_3

High-resolution Fourier transform absorption spectra of ozone in the 9-11 μm region have been recorded and analyzed by the group at NASA Langley and the College of William and Mary. Agreement of initial analyses shows good agreement with the intensities currently in HITRAN. However, analyses revealed that many air-broadened coefficients are significantly smaller than those in HITRAN. More air-broadened spectra have been recorded down to 165K and are currently being analyzed for broadening and shift coefficients for lines in the ν_3 band.

On the basis of measurements by Birk et al (M. Birk, G. Wagner, J.M. Flaud, and D.

Hausamann, "Line strengths in the ν_3-ν_2 hot band of ozone," *J.Molec.Spectrosc.* **163,** 262 (1994)), we plan to multiply the intensities of all lines in both the ν_3-ν_2 and ν_1-ν_2 hot bands in the far-IR by 1.23 for the next edition of HITRAN.

2.4. Nitrous oxide, N_2O

No new data for nitrous oxide have been added to HITRAN during this reporting period. The previous update included a revision and improvement for the pure rotation, the 17-μm region, and the 3-μm band system. The pure rotation was assimilated from the SAO database, while the IR regions come from the extensive work of R.A. Toth. On the other hand, parameters exist for the ν_2 band (580-670 cm^{-1}) and associated hot bands, (J.W.C. Johns, Z. Lu, M. Weber, J.M. Sirota, and D.C. Reuter, "Absolute intensities in the ν_2 fundamental of N_2O at 17 μm," *J.Mol.Spectrosc.* **177**, 203-210 (1996); M. Weber, J.M. Sirota, and D.C. Reuter, "l-resonance intensity effects and pressure broadening of N_2O at 17 μm," *J.Mol.Spectrosc* **177**, 211-220 (1996)) based on new laboratory measurements. These parameters will be incorporated in a future HITRAN release. The analysis contains Herman-Wallis factors that are not included in the current HITRAN study, where strengths are in error by up to 25% at higher *J*.

There was an anomaly discovered in the current database: the R3 line of the ν_2 fundamental of the principal isotope was inadvertently omitted. This situation will be corrected.

2.5. Methane, CH_4

A comprehensive revision of methane parameters is in progress at the University of Bourgogne in Dijon, France. In the region of the lowest fundamentals of CH_4 (900 - 2000 cm^{-1}), improved parameters are now available from the modeling of some 1700 observed line intensities for 9 hot bands (O. Ouardi, J.C. Hilico, M. Loëte, and L.R. Brown, "The hot bands of methane between 5 and 10 μm," *J.Mol.Spectrosc.* **180**, 311-322 (1996)) combined with the analysis of upper state levels near 3000 cm^{-1} (J.C. Hilico, J.P. Champion, S. Toumi, V.G. Tyuterev, S.A. Tashkun, "New analysis of the pentad system of methane and prediction of the (pentad-pentad) spectrum," *J.Mol. Spectrosc.* **168**, 455-476 (1994)) to determine the hot-band positions. New (but still preliminary) predictions of the 2000 to 3300 cm^{-1} and 3500 to 4700 cm^{-1} regions have been made

(J.C. Hilico, Université de Bourgogne, France, private communication). For $^{12}CH_3D$, new studies that are in progress are expected to provide complete predictions up to 3300 cm^{-1}. A new analysis of the triad (ν_6, ν_3, and ν_5) between 900 and 1700 cm^{-1} (A. Nikitin, J.P. Champion, Vl.G. Tyuterev, and L.R. Brown, "The high resolution spectrum of CH_3D in the region 900-1700 cm^{-1}," *J.Mol.Spectrosc.* **184,** 120-128 (1997)) has produced a new prediction with line positions improved by almost an order of magnitude.

L.R. Brown of JPL is also working on the 2.2- to 2.6-μm region in support of **MOPPIT** and these data will be incorporated into HITRAN in the future.

2.6. Oxygen, O_2

Oxygen was totally revisited for the 1996 HITRAN database. The best available constants for energy levels, positions, intensities, and halfwidths were selected and applied to the magnetic-dipole and electric-quadrupole transitions contained in HITRAN. Four different electronic states are represented. A reprint of a paper on the effort, which appeared during this reporting period, is enclosed.

However, soon after the database was released, two new independent measurements of the $a^1\Delta$ band at 1.27 μm were becoming available. The results were from W.J. Lafferty at NIST and D. Newnham of the Rutherford Appleton Lab in the UK. Their preliminary results for intensities agree within a few percent, but differ from the most recent HITRAN values by about 15%. They do show that at least HITRAN96 was an improvement over the prior databases. This band has been used as a benchmark for obtaining ozone profiles, so that having the best accuracy possible for the parameters is imperative. Before the two most recent observations, there was a lack of data on the absolute intensity of the band, and the three values that were obtainable in the literature differed substantially as well as containing large errors in the derivations.

We are also communicating with L.R. Brown of JPL who is making measurements of the intensities, wishes, and shifts of the A-band (0.762 μm) for **SAGE III.**

2.7. Nitric oxide, NO

An extensive update of nitric oxide was made for the current HITRAN edition. The update

came from two sources: a detailed work for the fundamental (1-0) band and the main branch (2-1) band compiled by V. Dana of France which included hyperfine splitting; and the hotter sequence of $\Delta v = 1$ bands as well as the overtone band sequence $\Delta v = 2$ compiled by Linda Brown from work done at the University of Denver and NASA. Other bands were left unchanged. Thus, there was a situation of at least three independent works contributing to the current edition.

Problems surfaced immediately, including a setback with respect to halfwidths for the fundamental bands. This situation is being remedied.

2.8. Sulfur dioxide, SO_2, and Nitrogen dioxide, NO_2

Interaction is continuing with A. Perrin of the University of Paris-South, France for improvements to both sulfur dioxide and nitrogen dioxide parameters. Her group, in collaboration with W. Lafferty of NIST have made significant recent updates to HITRAN for these molecules. Intensity improvements and accounting for resonances are a major part of the current effort to improve these parameters.

2.9. Nitric acid, HNO_3

Several recent and ongoing lab efforts have been dedicated to more accurate and consistent determination of the absolute band intensities in ν_2, ν_3, ν_4 and ν_5, $2\nu_9$ regions. Comparisons show significant inconsistencies in the laboratory measurements and improper hot-band correction for the 11-μm (ν_5,$2\nu_9$) and 7.6-μm (ν_3,ν_4) bands, while good consistency for the 5.8-μm (ν_2) bands. The work is not complete, and the recommendation adopted for the 1996 HITRAN, was to normalize to Giver et al (L.P. Giver, F.P.J. Valero, D. Goorvitch, and F.S. Bonomo, "Nitric-acid band intensities and band-model parameters from 610 to 1760 cm^{-1}," *J.Opt.Soc.Am.* **B1**, 715-722 (1984)) with the proper hot band correction, using $Q_V = 1.304$ at 296K. Thus, the ν_5, $2\nu_9$ lines of Perrin et al (A. Perrin, V. Jaouen, A. Valentin, J.-M. Flaud, and C. Camy-Peyret, "The ν_5 and $2\nu_9$ bands of nitric acid," *J.Mol.Spectrosc.* **157**, 112-121 (1993)) are normalized to Giver et al, without the hot bands, while the 11-μm obsolete hot bands are still in the database.

The ν_3 and ν_4 band line parameters in the 1992 HITRAN, were taken from A. Perrin, O. Lado-Bordowsky, and A. Valentin, "The ν_3 and ν_4 interacting bands of HNO_3 line positions and line

intensities," *Mol.Phys.* **67**, 249-270 (1989) and normalized approximately to the intensity measurements of R.D. May and C.R. Webster, "Measurements of line positions, intensities, and collisional air-broadening coefficients in the HNO_3 7.5-μm band using a computer controlled tunable diode laser spectrometer," *J.Mol.Spectrosc.* **138**, 383-397 (1989). The subsequent work of Perrin et al (A. Perrin, J.-M. Flaud, C. Camy-Peyret, V. Jaquen, R. Farrenq, G. Guelachvili, Q. Kou, F. Le Roy, M. Morillon-Chapey, J. Orphal, M. Badaoui, J.-Y. Mandin, and V. Dana, "Line intensities in the 11 - and 7.6-μm bands of HNO_3," *J.Mol.Spectrosc.* **160**, 524-539 (1993)) discusses some of the standing theoretical difficulties in the analysis of these bands, and provide a new normalization of the same line parameters, with a different intensity ratio of ν_3 to ν_4 bands, that has not been implemented for the 1996 database.

Clearly substantial progress has been made in HITRAN for the nitric acid bands as evidenced by the improving success in using the parameters for simulation of balloon-borne observations. Nonetheless, it remains a problem that must be carefully managed.

2.10. Trace constituents, H_2O_2 and HO_2

Two files of replacement data for hydrogen peroxide (H_2O_2) were received from the University of Paris (A. Perrin). These data, covering the far IR and 7.9-μm region, represent the torsion-rotation band and the ν_6, respectively. The Fourier transform spectra were recorded in Giessen, Germany; Florence, Italy; the University of Denver; and in Paris. They are not in the HIITRAN format and must be examined and validated.

A new set of HO_2 parameters was obtained from K. Chance of SAO. These are new pure rotational lines that will be assessed for replacement on HITRAN.

2.11. IR Cross-sections

The increased use of hydrofluorocarbons (HFCs), which are expected to replace CFCs and HCFCs in many applications in order to reduce the deleterious effects of released chlorine on the atmospheric ozone layer, will add another absorber in the IR "window" region, 8-12 μm. IR cross-sections were obtained for HFC-134 (CHF_2CHF_2) and HFC-143a (CF_3CH_3) which are new species for HITRAN. These data came from the joint collaborative work of K. Smith at Strathclyde

University in Glasgow and D. Newnham of the Rutherford Appleton lab. The latest cross-section data for the HCFCs have been archived and placed on the HITRAN web-site.

Visits to the laboratory of Prof. P. Varanasi at SUNY Stony Brook, NY have been made to discuss replacements for cross-sections such as CCl4, and also to remove outdated, inconsistent cross-sections, such as some of the CFC-11 and CFC-12 data that have been replaced by the data sets of his laboratory.

3. HAWKS Software Development, Upgrades, and Distribution

Development of the full featured version of HAWKS continued. Sorting and Merge options were completed and work well. The graphing option has been added as a separate thread. Tests show that the graphing operates at about the same speed as the MS Windows version. The SELECT process has been moved to a separate thread to give the Java HAWKS a smoother operating interface. The Ontar Corp continued to develop features for HAWKS. PDF file format was chosen for the printing of selections from HITRAN. HITRAN help was also set up. The Ontar Corp completed the BAND STATS section of HAWKS. "Band Stats" is the utility in the software that enables the user to determine extrema for different parameters of each molecular band in HITRAN. This tool is extremely useful for the contributors to HITRAN quickly to authenticate additions, updates, and consolidation to the database. It enables users to obtain a quick view of bands and to compare with previous editions of the database. However, we have been disappointed in the performance at this time of the Java version. The slowness is due to the interpretive nature of the language, which hopefully will change as the language gains wider use and develops. The Ontar Corp investigated the use of a better method for making a help system for HAWKS, testing the HTML Java Bean.Developed a Windows95 and WindowsNT installation program for Java HAWKS. The installation programs install the Java Runtime Environment 1.1.3 (JRE1.1.3). The JRE allows users to install Java HAWKS on computers that do not have a Java VM already installed.

Several users informed us of problems with the temperature scaling in the current HAWKS. On the 1996 current edition, if partition sum information was not available for an isotope, the HAWKS software eliminates the output for temperatures other than the standard 296K. We should at least use the routine that Rothman developed for FASCODE in these cases, i.e., scale the ratio of

the partition sums to be proportional to the 3/2 or unity power of the temperature ratios. The applicable domains of our approach, and the temperature ranges, are being explained in the definitive HITRAN article. Some errors in the calculation of the partition sum for the doublet-pi molecules (NO, OH, ClO) were discovered and are being corrected. An article is in preparation.

A test copy of the future HAWKS CD-ROM was created. This version incorporates the updates to carbonyl sulfide (OCS), the HOBr relegated previously to the supplemental directory, and the new ethylene data. In addition, the new JAVA software has been included. We feel that the next version of documentation should be in the PDF format, rather than having WORD and WordPerfect files as in the last public edition of HAWKS.

Various minor typos and errors were corrected on the HAWKS software. A readable form of the HITRAN database (decoding of the quantum identifications and more space between parameters) has been added as an output option in addition to the direct image of the database after filtering (the latter output is used subsequently by programs, the former is more useful for visual examination purposes).

A new feature was added to the HAWKS software to enable it to plot the cross-section data in the compilation. Testing indicated that it would be good to add the option to plot the points, as well as histograms. This implementation will enable us to more easily make comparisons of various pressure-temperature cross-sections (which we have designated as "panels").

We worked on JAVA development for the MAC version of HAWKS. Ontar developed applets and software filtering, but found difficulty in implementing a simple installation setup. Help was available from R. Plume of the SAO who wrote an elaborate script for this procedure.

4. HITRAN Web-site Development

During this period we placed C_2H_4 line parameters and a total replacement for OCS on the web-site. Ethylene represents a new species for HITRAN. The OCS data that we obtained from Andre Fayt's group in Belgium was quite extensive, and well beyond the expected needs of HITRAN users. We decided to retain transitions that were basically within the dynamic range of previous carbonyl sulfide data in HITRAN. These parameters have been amalgamated with the pure rotation bands already existing in HITRAN to form a complete set that is available on the HITRAN

web-site to form a complete replacement for OCS. It should be remarked that an additional isotopomer is now included for the first time, namely $^{16}O^{12}C^{33}S$ (623 in AFGL code). In keeping with the HITRAN system of numbering isotopes sequentially based on terrestrial abundances, the isotope $^{18}O^{12}C^{32}S$ (822) which has been labeled 4 including the current edition of HITRAN, becomes number 5 hereafter.

We also updated the file MOLPARAM.TXT to include the increased number of isotopes and species and placed it on the UPDATE page of the HITRAN web-site. This file contains valuable information not included in the line-by-line portion of HITRAN, namely the statistical weights of the species and their isotopes, the value of the total internal partition sum at 296K, the molecular weights, and the abundances.

5. Collaborations

Joined in an international collaborative effort to propose to the Commission of the European Community a program, Spectroscopic Data Base for Atmospheric Satellite Experiments (SDBASE). The general goals of this program will be to provide a sufficient database for modeling of the stratospheric chemistry and assist in the retrieval of trace gas distributions from the MIPAS (**M**ichelson **I**nterferometer for **P**assive **A**tmospheric **S**ounding) and SCIAMACHY (**SC**anning **I**maging **A**bsorption **S**pectro**M**eter for **A**tmospheric **CH**artograph**Y**). The project includes representatives of government and university laboratories in Germany, Italy, France, Belgium, and the US. However, it was discovered that the European Commission cannot fund US representatives. Nonetheless, participation in this program, at least at the consulting level, would be very beneficial to the NASA EOS program and HITRAN, especially since new and improved data will be deposited in the HITRAN database.

6. Meetings, Presentations, and Publications

Presented paper "Computational Methods Applied to the Development of HITRAN and HITEMP," at the DoD Transmission Meeting, AF Geophysics Directorate, Hanscom AFB, Massachusetts (June 1997).

Attended the 52nd International Molecular Spectroscopy Symposium, Ohio State University,

Columbus, Ohio (June 1997). Chaired Infrared Session that consisted of 15 contributed papers.

High-Resolution Spectroscopy Meeting: Attended the Fifteenth Colloquium on High Resolution Molecular Spectroscopy, at Strathclyde University, Glasgow, UK, September 1997. Presented a poster: "Global Fitting of CO_2 Vibrational-Rotational Lines using the Effective Hamiltonian Approach," (with S.A. Tashkun, V.I. Perevalov, J.-L. Teffo, D. Bailly, and Vl.G. Tyuterev).

This conference also offered the opportunity to have a meeting with members of the SDBASE group. Key species were identified that need to be improved or added to HITRAN. These include $ClONO_2$ (chlorine nitrate), HNO_3 (nitric acid), NO_2 (nitrogen dioxide), H_2O, O_3, ClOOCl (chlorine peroxide), and CH_3Br (methyl bromide). These species strongly influence the amount of ozone in the stratosphere by means of homogeneous and heterogeneous chemical processes.

During this reporting period, the Special Issue "Atmospheric Spectroscopy Applications 96", of the Journal of Quantitative Spectroscopy and Radiative Transfer (*JQSRT*) Volume 59, number 3-5 March-May (1998) appeared. The ASA Special Issue was co-edited by L.S. Rothman with A. Barbe of the University of Reims in France and contains numerous articles on the six topics covered in the last ASA meeting (Non-LTE, databases, continua and lineshape, experiments, lab efforts, and techniques). The paper, "Improved Spectral Parameters for the Three Most Abundant Isotopomers of the Oxygen Molecule," R.R. Gamache, A. Goldman, and L.S. Rothman, *JQSRT* **59,** 495-509 (1998) appeared in this issue.

HITRAN *JQSRT* Special Issue: A major effort has gone into the HITRAN Special Issue. The guest editors are L.S. Rothman, C.P. Rinsland (NASA Langley), and A. Goldman (Univ. Denver). Eighteen papers are expected, and at the time of this reporting period 15 had been sent out to two referees each. Besides the HITRAN lead-off paper, there are papers dealing with state-of-the-art parameters for water vapor, carbon dioxide, ozone, carbon monoxide, NO, NO_2, SO_2, HNO_3, HBr, $ClONO_2$. There are also papers describing related databases: the JPL catalog, HITEMP, and the SAO Solar line Atlas. A pair of papers completes the edition, describing ATMOS/ATLAS infrared measurements in the tropical and subtropical upper atmosphere. I was a coauthor on the following papers:

"The HITRAN Molecular Spectroscopic Database and HAWKS (HITRAN Atmospheric Workstation): 1996 Edition," L.S. Rothman, C.P. Rinsland, A. Goldman, S.T. Massie, D.P. Edwards, J.-M. Flaud, A. Perrin, C. Camy-Peyret, V. Dana, J.-Y. Mandin, J. Schroeder, A. McCann, R.R. Gamache, R.B. Wattson, K. Yoshino, K. Chance, K. Jucks, L.R. Brown, V. Nemtchinov, and P. Varanasi;

"High-temperature Spectrum of H_2O in the 720 to 1400 cm^{-1} Region," M.P Esplin, R.B. Wattson, M.L. Hoke, and L.S. Rothman; and

"Global Fitting of $^{12}C^{16}O_2$ Vibrational-Rotational Line Positions Using the Effective Hamiltonian Approach," S.A. Tashkun, V.I. Perevalov, J.-L. Teffo, L.S. Rothman, and Vl.G. Tyuterev.

I am on the international committee of International Conference on Water in the Gas Phase (WGP 98). This conference will convene many of the world's experts on the research of water (topics include the spectroscopy of water, clusters, the structure and dynamics, and ionic forms of water vapor). The meeting will take place in June at the University of Marne-la-Vallée, outside Paris.

ARM Science Team Meeting: Attended the ARM Science Team meeting in Tucson, Arizona in March. A poster was presented showing recent enhancements to HITRAN for the ARM program. A focus was on recent progress in providing modeling capabilities for the hydrofluorocarbons (HFCs). The meeting also provided the opportunity to meet with various members of the **EOS** program: had discussions with Frank Murcray of the University of Denver concerning the **SAGE** program, met with David Starr to discuss progress and directions of the HAWKS program as related to EOS, and communicated with various participants in the ARM program whose efforts overlap concerns of EOS.

Meeting at JPL: Following the ARM Science Team meeting, traveled to JPL in Pasadena where a meeting was arranged by Reinhard Beer. Participating were Ming Luo (**TES** level-2 retrieval), Helen Worden, and Kevin Bowman. Helen described an HNO_3 problem, where they still are relying on the Hanst data. They are interested in heavier hydrocarbons, and acetone, isoprene, butane, propane, formic acid, formaldehyde, methanol, and ethane. Cross-sections as have been introduced into HITRAN would be sufficient. However, HITRAN has initiated formic acid and

ethane as line-by-line parameters, but these need extensive improvements. Improvements in water vapor self-broadening coefficients as well as line shifts would be desirable in the next HITRAN edition. **TES** would also profit from the addition of line-coupling capabilities planned for future HITRAN editions. Methyl bromide (CH_3Br) in the 600 to 3050-cm^{-1} region is also desired. This molecule is not presently included in HITRAN.

While at JPL, had meetings with Linda Brown and Ed Cohen. We discussed the status of HDO pure rotation and the 1600-cm^{-1} region that is being worked on by Bob Toth in collaboration with Laurent Coudert (Laboratoire de Photophysique Moléculaire, Bât.210, Université Paris-Sud, 91405 Orsay, France). Linda also described the status of new methane parameters: the 3 to 5-μm region is in progress and is of concern to **TES**; the 2 to 3-μm region only has the principal isotope and is of concern to **MOPPIT**; new work will be coming in the 1.6 to 2-μm region, useful for laser efforts. There is the prospect of a new replacement list for HITRAN for ammonia in the 3000 to 3800 cm^{-1} region as well as a joint analysis with Isabel Kleiner (Laboratoire de Photophysique Moléculaire, Bât.210, Université Paris-Sud, 91405 Orsay, France) that is being done in the 5 to 8-μm region. A linelist for methyl chloride (CH_3Cl) between 1200 and 1700 cm^{-1} is almost ready; this would represent a significant improvement for HITRAN. Linda is making measurements at Kitt Peak on the oxygen A-band, particularly line positions, air- and self-broadening coefficients, shifts, and the temperature dependence of halfwidths; we are keeping abreast of these developments. Finally, she expects to be able to compare the 9000 to 15000-cm^{-1} region data we have for water vapor with the recent calculations of David Schwenke of NASA Ames.

VOLUME 59 NUMBER 3–5 MARCH–MAY 1998 ISSN 0022-4073

Journal of Quantitative Spectroscopy & Radiative Transfer

SPECIAL ISSUE

ATMOSPHERIC SPECTROSCOPY APPLICATIONS 96

Guest Editors:

A. Barbe
M. F. Mérienne
L. S. Rothman

PERGAMON

ATMOSPHERIC SPECTROSCOPY APPLICATIONS 96

Guest Editors:

A. Barbe

M. F. Mérienne

Group de Spectrométrie
Moléculaire et Atmosphérique, France

L. S. Rothman

Harvard–Smithonian Center for Astrophysics Atomic
and Molecular Physics Division, U.S.A.

PERGAMON

Pergamon

J. Quant. Spectrosc. Radiat. Transfer Vol. 59, No. 3–5, p. vii, 1998
Published by Elsevier Science Ltd. Printed in Great Britain
0022-4073/98 $19.00 + 0.00

PREFACE

The papers in this Special Issue of the *Journal of Quantitative Spectroscopy and Radiative Transfer* (*JQSRT*) are derived from the *Fourth Conference on Atmospheric Spectroscopy Applications* (ASA). This conference, under the auspices of the International Radiation Commission (IRC) and the International Ozone Commission (IOC), has taken place every third year. The fourth conference, like the previous one, was held in Reims, France (4–6 September 1996). A Special Issue of *JQSRT* (Volume 52, September/October 1994) also arose from the previous conference, and a brief history of the ASA working group is given in the Guest Editorial of that issue.

More than 130 people from around the world participated in the fourth conference. An emphasis this time was on posters presentations in order to allow for more periods of dialogue. There were six invited speakers, each giving an overview of one of the six principal topics of ASA, and four shorter oral communications during the database session. The Proceedings that came out of this conference contains 86 papers.

It is our experience that in the field of spectroscopy, and especially with its applications to atmospheric studies, new ideas and results often come to fruition in two years; thus the papers in this issue represent new results and thrusts that were not available at the last convening. In keeping with the framework of ASA, we have maintained the six principal topics of the working group: (1) laboratory data; (2) atmospheric observations; (3) lineshape and continua; (4) techniques; (5) non-local thermodynamic equilibrium; and (6) databases. The 28 papers and one note in this issue are fairly well distributed over the topics under consideration by ASA. The issues covered in these papers are ones of great concern as we enter an era of promising global coverage of the atmosphere by satellites. These sophisticated experiments require a good spectroscopic understanding and modeling capability, as well as reliable validation tools, if they are to accomplish their goals of remote sensing.

We wish to express our deep appreciation for the invaluable help and assistance in the preparation of this Special Issue and the success of the ASA meeting to J.-M. Flaud, R. R. Gamache, A. Goldman, R. Tipping, P. Varanasi, and R. Zander. We also would like to acknowledge the support of the University of Reims Champagne Ardenne, the city of Reims, le Ministère de l'Education Nationale de l'Enseignement Supérieur et de la Recherche, and to the CNRS (Centre National de Recherche Scientifique) of France.

A. BARBE
M. F. MÉRIENNE
L. S. ROTHMAN
Guest Editors

CONTENTS

ATMOSPHERIC SPECTROSCOPY APPLICATIONS 96

SECTION A—LABORATORY DATA

SECTION B—ATMOSPHERIC OBSERVATIONS

SECTION C—LINESHAPES/CONTINUA

PERGAMON

ISSN 0022-4073
JQSRAE 59(3–5) 137–528 (1998)

PERGAMON

ISSN 0022-4073
JQSRAE 59(3–5) 137–528 (1998)

Pergamon

J. Quant. Spectrosc. Radiat. Transfer Vol. 59, No. 3–5, pp. 495–509, 1998

Printed in Great Britain
PII: S0022-4073(97)00124-6
0022-4073/98 $19.00 + 0.00

IMPROVED SPECTRAL PARAMETERS FOR THE THREE MOST ABUNDANT ISOTOPOMERS OF THE OXYGEN MOLECULE

ROBERT R. GAMACHE,†‡ AARON GOLDMAN§ and LAURENCE S. ROTHMAN‖

†Department of Environmental, Earth, and Atmospheric Sciences, University of Massachusetts Lowell, 1 University Avenue, Lowell, MA 01854, U.S.A., §Department of Physics, University of Denver, Denver, CO 80208, U.S.A. and ‖AF Geophysics Directorate, 29 Randolph Road, Hanscom AFB, Hanscom, MA 01731, U.S.A.

Abstract—Line positions, intensities, transition-moment squared, and lower state energies are calculated for the three most abundant isotopomers of the oxygen molecule in the terrestrial atmosphere, $^{16}O_2$, $^{18}O^{16}O$, and $^{17}O^{16}O$. All lines passing a wavenumber dependent cutoff procedure (3.7×10^{-30} cm^{-1}/(molecule cm^{-2}) at 2000 cm^{-1}) are retained for the 1996 HITRAN database. Halfwidths as a function of the transition quantum numbers are determined from the available experimental measurements. Explicit expressions are obtained relating line intensities to the transition-moment squared, the vibrational band intensity, and the electronic-vibrational Einstein-A coefficient. The statistical degeneracy factors are presented and misuse of these factors in previous works is explained. Finally, band-by-band comparisons between the new calculations and the data from the previous HITRAN database are made. © 1998 Elsevier Science Ltd. All rights reserved

1. INTRODUCTION

Atmospheric spectra of oxygen are used for deducing information about properties and other species in the atmosphere, for example, measurements of O_2 emission are used as a standard for O_3 profile analysis.[1,2] There is a need to have available the most accurate parameters for this molecule. The spectrum of the oxygen molecule, even though O_2 is a simple diatomic, is unexpectedly complex. The oxygen molecule has two unpaired electrons with a total spin of 1 in the electronic ground state. There are two low-lying excited electronic states which give rise to near-I.R. and visible spectra, and the symmetries of the isotopomers, $^{16}O_2$, $^{16}O^{18}O$, and $^{16}O^{17}O$, affect the number of allowed states. In addition, both magnetic dipole and electric quadrupole transitions occur, the degeneracy of states needs to be carefully considered, and transitions occur from the microwave to the visible. Although the line intensities are usually small, the high mixing ratio and long optical path in the terrestrial atmosphere compensate to produce meaningful absorption.[3]

In this work, the spectral parameters for the oxygen molecule are calculated for the electronic-vibrational bands listed in Table 1. These data represent an improvement to the data contained on the 1992 version of the HITRAN molecular absorption database,[4] which are from calculations made in 1982.[5] The calculations consider the lower state energy, the wavenumber of the transition, the line intensity, and transition moment squared of the spectral lines. In addition, halfwidths as a function of transition quantum number are determined from the available experimental measurements. All fundamental physical constants used in the calculations are those reported by Cohen and Taylor.[6] The calculations were made in double precision on several different computer systems using codes written in FORTRAN. Below, we discuss the theory of molecular oxygen and describe the improvements to the data for each band.

‡To whom all correspondence should be addressed.

Table 1. Electronic-vibrational bands of O_2 from 0 to 16,000 cm^{-1}

Electronic band	Isotopomer $^{16}O_2$ $v' \leftarrow v''$	$^{16}O^{18}O$ $v' \leftarrow v''$	$^{16}O^{17}O$ $v' \leftarrow v''$
$X^3\Sigma_g^- \leftarrow X^3\Sigma_g^-$	0←0	0←0	0←0
	1←0		
	1←1		
$a^1\Delta_g \leftarrow X^3\Sigma_g^-$	0←1	0←0	
	0←0		
	1←0		
$b^1\Sigma_g^+ \leftarrow X^3\Sigma_g^-$	0←0	0←0	
	1←0	1←0	1←0
	2←0	2←0	
	1←1		
	0←1		

2. GENERAL THEORY

To understand the spectrum of the molecular oxygen in the atmosphere, one must consider the properties of the three most abundant isotopic species of oxygen and the structure of the three lowest-lying electronic states. An excellent review for this material can be found in Herzberg.[7,8]

The theoretical treatment of the ground state of molecular oxygen was first given by Tinkham and Strandberg[9] and it was later clarified with the aid of the transformation theory of spherical tensors by Steinbach and Gordy.[10,11] References 12 and 13 give excellent overviews of the theory. The ground electronic state of the oxygen molecule is the $X^3\Sigma_g^-$ state. There are also two low-lying electronic states, the $a^1\Delta_g$ state and the $b^1\Sigma_g^+$ state at 7918 cm^{-1} and 13 195 cm^{-1} above the ground state, respectively. Since the electronic ground state is the $X^3\Sigma_g^-$ state, the average electronic orbital angular momentum vanishes ($\Lambda = 0$). Still there is an instantaneous non-zero value of the orbital angular momentum which produces a precessing magnetic dipole moment of orbital origin. The total electronic spin is $S = 1$, so that molecular oxygen has a permanent magnetic dipole moment of approximately two Bohr magnetons. The energy is described in terms of the total electronic spin vector, **S**, and the rotational angular momentum, **N**. In the electronic ground state, Hund's coupling case (b) dominates[7] (more recent work shows the need for intermediate coupling) and the total angular momentum **J** is $\mathbf{J} = \mathbf{N} + \mathbf{S}$. Thus for each value of N there are 3 allowed values of J. The oxygen molecule can interact with an electromagnetic field via its magnetic dipole (md) moment or by its electric quadrupole (eq) moment. In this work, calculations are made for both md and eq lines of O_2.

The principal isotopic species, $^{16}O_2$, is unique in that it is the only homonuclear diatomic molecule of the three isotopomers on the database. Because of this symmetry and the fact that the oxygen-16 nuclei have zero nuclear spin, the molecule behaves as a Bose particle. Thus the total wavefunction must be symmetric with respect to inversion through the center. The spins of the individual electrons form a resultant $S = 1$ that gives rise to a coupling of electronic (S) and rotational angular momentum (N) yielding a triplet of states labeled by J; $J = N$, $J = N + 1$, and $J = N - 1$. The wavefunctions for the vibrational and nuclear motion are symmetric, whereas the electronic wavefunction for a Σ_g^- state is antisymmetric, indicating the only allowed rotational wave functions are those for odd (antisymmetric) N. The result is that half (all N even) of the states of $^{16}O_2$ are missing in the ground electronic state.

In the $a^1\Delta_g$ electronic state, the resultant of the individual electron spin is zero ($S = 0$) giving $J = N$, but the rotational levels are split into two, one symmetric (+) and one antisymmetric (−) state, by Λ-doubling. Because of the constraints placed on the wavefunction by Bose–Einstein statistics, only the (+) state is allowed and, although all N are occupied, only half the states are realized. The $b^1\Sigma_g^+$ electronic state also has $S = 0$ giving $N = J$ and the electronic wavefunction for the Σ_g^+ state is symmetric as are Ψ_{nuc} and Ψ_{vib}; thus the only rotational wavefunctions are the symmetric (N even) ones. Because of the symmetry of the $^{16}O_2$ species and the nuclear spin $I(^{16}O) = 0$, half of the rotational states of *each* electronic level are missing.

For the two isotopic species on the database, $^{16}O^{18}O$ and $^{16}O^{17}O$, inversion, through the center is no longer a valid symmetry operation. For this condition, all rotational levels of the molecule are allowed, both (+) and (−). The ground electronic state is a triplet, $J = N$ and $J = N \pm 1$,

with all N allowed, $N = 1, 2, 3, \ldots$. The two low-lying electronic states, $a^1\Delta_g$ and $b^1\Sigma_g^+$ are singlets ($J = N$) with all values of N (even and odd) starting at $N_{min} = \Lambda$. Note that for the $a^1\Delta_g$ state there is Λ-type doubling, thus each N has two states.

Figure 1 is a rotational state diagram for the lowest three electronic states of O_2. A note of caution here: the rotational states of a diatomic molecule are classified according to the behavior of the *total wavefunction* with respect to reflection at the origin and not of the rotational wavefunction alone (see pp. 128–129 of Ref. 7). Thus in the diagram, the states labeled (+) in the $X^3\Sigma_g^-$ state correspond to N = odd (antisymmetric) states; whereas the states labeled (+) in the $b^1\Sigma_g^+$ state correspond to N = even (symmetric) states. The principal species of oxygen, $^{16}O_2$, follows Bose–Einstein statistics and as such does not have any of the (−) symmetry levels. Thus in the diagram all (−) states are eliminated, in the $X^3\Sigma_g^-$ state all even N levels are missing, in the $a^1\Delta_g$ state one level for each N is missing, and in the $b^1\Sigma_g^+$ state all odd N are missing. For the non-homonuclear species all levels are allowed. These symmetry factors have an important role in the statistics of the molecular. Taking the ratio of the number of levels in the $X^3\Sigma_g^-$ state to the $a^1\Delta_g$ state gives 3:2 regardless of the isotopomer (this is because for $^{16}O_2$ half the levels are missing in each electronic state). Likewise the similar ratio of the $X^3\Sigma_g^-$ state to the $b^1\Sigma_g^+$ state is 3:1.

3. LINE INTENSITIES

Various formulas are used to calculate the line intensities depending on the particular transition. Below these formulas are presented along with other relationships needed for the calculations. Also presented are relationships to explain problems encountered in determining the Einstein-A coefficients for transitions in the $X^3\Sigma_g^- \rightarrow a^1\Delta_g$ band. The transitions involve, in general, different electronic, lambda doubling, vibrational, and rotational states which will be labeled by ε,Λ,v, and (J,M), respectively with the usual spectroscopic notation of a single prime for the upper state and a double prime for the lower state. In the absence of an electric or magnetic field, the M states are degenerate and will be summed over to express the line intensity for the transition labeled by $\varepsilon''\Lambda''v''J'' \rightarrow \varepsilon'\Lambda'v'J'$. In the following, a shorthand notation will be adopted by substituting η for

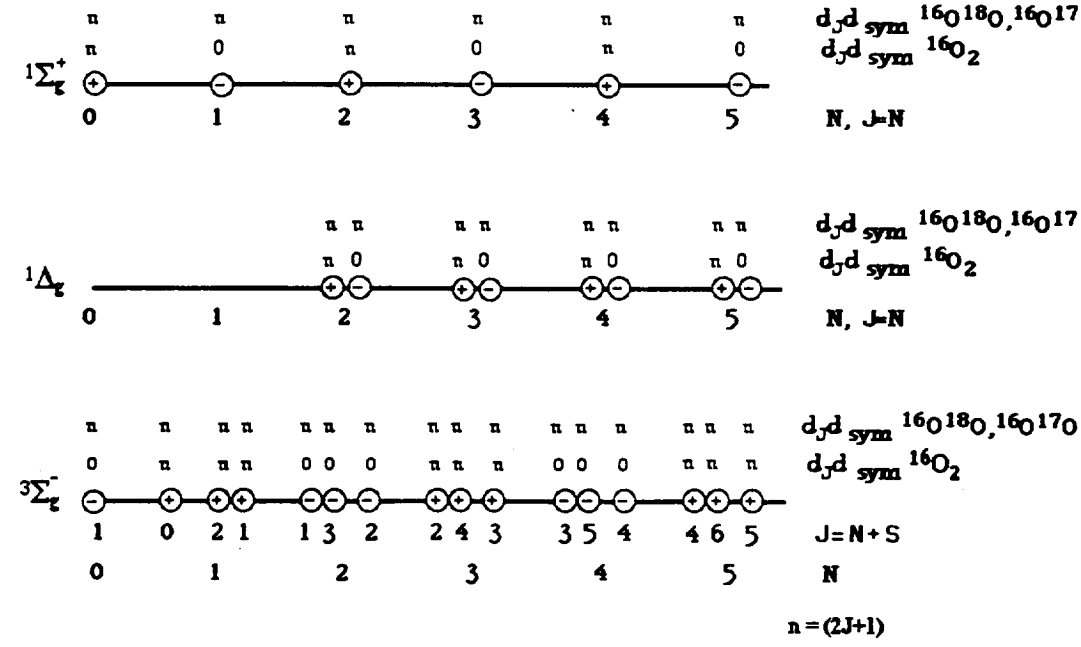

Fig. 1. State diagram for the three lowest electronic levels of the oxygen molecule, $X^3\Sigma_g^-$, $a^1\Delta_g$, and $b^1\Sigma_g^+$, and their statistical weights.

the set of quantum numbers $\varepsilon\Lambda vJ$. Thus $\eta'' \equiv \varepsilon''\Lambda''v''J''$ and $\eta' \equiv \varepsilon'\Lambda'v'J'$. The line intensity in units of (cm^{-1}/molecule cm^{-2}) for a transition $\eta'' \rightarrow \eta'$ is (see Refs. 14 and 15)

$$S_{\eta''\rightarrow\eta'} = \frac{8\pi^3}{3hc} I_a \frac{(d_{\eta''} e^{-E_{\eta''}/kT})}{d_{J''} Q(T)} \frac{\nu_{(\eta'')(\eta')}}{c} \left(1 - e^{-h\nu_{(\eta'')(\eta')}/kT}\right) \sum_{M'',M'} |R_{(\varepsilon''\Lambda''v''J''M'')(\varepsilon'\Lambda'v'J'M')}|^2 \, 10^{-36}, \quad (1)$$

where the total internal partition sum, $Q(T)$, is

$$Q(T) = \sum_{\varepsilon\Lambda vJ} d_\varepsilon d_\Lambda d_v d_J d_{sym} e^{-E_{\varepsilon\Lambda vJ}/kT}, \quad (2)$$

and I_a is the isotopic abundance of the species, the factor 10^{-36} is needed for the units chosen. $|R_{(\varepsilon''\Lambda''v''J''M'')(\varepsilon'\Lambda'v'J'M')}|^2$ is the transition-moment squared and has units of Debye^2/molecule, $d_{\eta''}$ is the degeneracy and $E_{\eta''}$ the energy of the state η'', $\nu_{(\eta'')(\eta')}/c = \omega_{(\eta'')(\eta')}$ is the wavenumber of the transition, and all other variables are the usual constants. (Note, in Eq. (1) and in a few expressions that follow we have not canceled some of the degeneracy factors in order to emphasize the fractional number of molecules in the state η'', $N_{\eta''}$.) In this paper we use the 'regular' matrix elements while in the Gamache and Rothman (1992) paper[15] we used the 'weighted' ones. The degeneracy factors are given by the product of the degeneracy factors for the quantized motions, $d_\eta = d_\varepsilon d_\Lambda d_v d_{sym}$ with $d_\varepsilon = (2S + 1)$, $d_\Lambda = (2 - \delta_{\Lambda,0})$, $d_v = 1$, $d_J = (2J + 1)$, and d_{sym} is one for the heteronuclear species and the (+) states of the homonuclear species and zero for the (−) states of the homonuclear species. This factor accounts for the symmetry restrictions for the homonuclear diatomics (note, this gives an overall factor of 1/2 in the partition sum).

This expression can be written in terms of the Einstein-A coefficient by making use of the relationship[14]

$$A_{\eta''\rightarrow\eta'} = \frac{64\pi^4 \, 10^{-36}}{3h} \omega^3_{(\eta'')(\eta')} \frac{1}{d_{J''}} \sum_{M'',M'} |R_{(\varepsilon''\Lambda''v''J''M'')(\varepsilon'\Lambda'v'J'M')}|^2, \quad (3)$$

whence the line intensity is

$$S_{\eta''\rightarrow\eta'} = \frac{I_a}{8\pi c} \frac{(d_{\eta''} e^{-E_{\eta''}/kT})}{Q(T)} \frac{1}{\omega_{(\eta'')(\eta')}} \left(1 - e^{-h\nu_{(\eta'')(\eta')}/kT}\right) \frac{d_{J'}}{d_{J''}} A_{\eta''\rightarrow\eta'}. \quad (4)$$

The Einstein-A coefficient is usually determined from a measurement of a vibrational band intensity, $S^{\varepsilon''\Lambda''v''}_{\varepsilon'\Lambda'v'}$ so it is useful to formulate Eq. (1) and Eq. (4) in terms of this quantity. The integrated intensity for an electronic-vibration–rotation band in units of cm^{-1}/(molecule cm^{-2}) is given by[14]

$$S^{\varepsilon''\Lambda''v''}_{\varepsilon'\Lambda'v'} = \frac{8\pi^3 \, 10^{-36}}{3hc} \omega_{\varepsilon''\Lambda''v''(\varepsilon'\Lambda'v')} \frac{(d_{\varepsilon''\Lambda''v''} e^{-E_{\varepsilon''\Lambda''v''}/kT})}{Q_{\varepsilon\Lambda v}} |R_{(\varepsilon''\Lambda''v'')(\varepsilon'\Lambda'v')}|^2. \quad (5)$$

(Note, this is similar to α/N_L (Ref. 14, p. 153 with $\alpha = \Sigma_{J''J'} S_{\varepsilon''\Lambda''v''J''\rightarrow\varepsilon'\Lambda'v'J'}$) with the exception that the radiation field term, $(1 - e^{-h\nu_{(\eta'')(\eta')}/kT})$, is explicitly retained in the rotational part of the intensity formula. Thus our definition of $S^{\varepsilon''\Lambda''v''}_{\varepsilon'\Lambda'v'}$ does not contain the approximate factor $(1 - e^{-h\nu_{(\varepsilon''\Lambda''v'')(\varepsilon'\Lambda'v')}/kT})$.) To implement Eq. (5), the electronic-vibration and rotation parts are separated using the product approximation for the total partition sum and the transition-moment squared, and the assumption of additivity of energy

$$Q_{tot} = Q_{\Lambda v} \cdot Q_{rot}, \quad (6)$$

$$\sum_{M'',M'} |R_{(\eta''\eta')}|^2 = |R_{(\varepsilon''\Lambda''v'')(\varepsilon'\Lambda'v')}|^2 \cdot |R_{(J'')(J')}|^2,$$

$$E_{\eta''} = E_{\varepsilon''\Lambda''v''} + E_{J''}.$$

Inserting these into Eq. (1) and rearranging terms yields

$$S_{\eta''\to\eta'} = \frac{8\pi^3\ 10^{-36}}{3hc} \frac{(d_{\varepsilon''\Lambda''v''} e^{-E_{\varepsilon''\Lambda''v''}/kT})}{Q_{\varepsilon\Lambda v}} \omega_{(\varepsilon''\Lambda''v'')(\varepsilon'\Lambda'v')} |R_{(\varepsilon''\Lambda''v'')(\varepsilon'\Lambda'v')}|^2 \tag{7}$$

$$\times I_a \frac{(d_J \cdot d_{sym} e^{-E_{J''}/kT})}{d_J \cdot d_{sym} Q_{rot}} \frac{\omega_{(\eta''\eta')}}{\omega_{(\varepsilon''\Lambda''v'')(\varepsilon'\Lambda'v')}} \left(1 - e^{-h\nu_{(\eta''\eta')}/kT}\right) |R_{(J'')(J')}|^2.$$

The first part of this expression is simply the band intensity as defined in Eq. (5); thus the line intensity can be written

$$S_{\eta''\to\eta'} = S^{\varepsilon''\Lambda''v''}_{\varepsilon'\Lambda'v'} I_a \frac{(d_J \cdot d_{sym} e^{-E_{J''}/kT})}{d_J \cdot d_{sym} Q_{rot}} \frac{\omega_{(\eta''\eta')}}{\omega_{(\varepsilon''\Lambda''v'')(\varepsilon'\Lambda'v')}} \left(1 - e^{-h\nu_{(\eta''\eta')}/kT}\right) |R_{(J'')(J')}|^2. \tag{8}$$

In what follows we will need the relationships between the Einstein coefficients and the electronic-vibrational transition-moment squared. They are

$$B_{\varepsilon'\Lambda'v'\to\varepsilon''\Lambda''v''} = \frac{8\pi^3\ 10^{-36}}{3h^2} |R_{(\varepsilon''\Lambda''v'')(\varepsilon'\Lambda'v')}|^2, \tag{9a}$$

$$B_{\varepsilon'\Lambda'v'\to\varepsilon''\Lambda''v''} = \frac{8\pi^3\ 10^{-36}}{3h^2} \frac{d_{\varepsilon''\Lambda''v''}}{d_{\varepsilon'\Lambda'v'}} |R_{(\varepsilon''\Lambda''v'')(\varepsilon'\Lambda'v')}|^2, \tag{9b}$$

and

$$A_{\varepsilon'\Lambda'v'\to\varepsilon''\Lambda''v''} = \frac{64\pi^4\ 10^{-36}}{3h} \omega^3_{(\varepsilon'\Lambda'v')(\varepsilon''\Lambda''v'')} \frac{d_{\varepsilon''\Lambda''v''}}{d_{\varepsilon'\Lambda'v'}} |R_{(\varepsilon''\Lambda''v'')(\varepsilon'\Lambda'v')}|^2. \tag{9c}$$

Solving Eq. 9c for the transition-moment squared and inserting into Eq. (5) gives the result

$$S^{\varepsilon''\Lambda''v''}_{\varepsilon'\Lambda'v'} = \frac{1}{8\pi c} \frac{(d_{\varepsilon''\Lambda''v''} e^{-E_{\varepsilon''\Lambda''v''}/kT})}{Q_{\varepsilon\Lambda v} \omega^2_{(\varepsilon'\Lambda'v')(\varepsilon''\Lambda''v'')}} \frac{d_{\varepsilon'\Lambda'v'}}{d_{\varepsilon''\Lambda''v''}} A_{\varepsilon'\Lambda'v'\to\varepsilon''\Lambda''v''}. \tag{10}$$

This expression allows the Einstein-A coefficient to be determined by measuring the integrated band intensity. This relationship with Eq. (8) allows the $\varepsilon''\Lambda''v''J''\to\varepsilon'\Lambda'v'J'$ line intensity to be written in terms of the Einstein $A_{\varepsilon'\Lambda'v'\to\varepsilon''\Lambda''v''}$ coefficient

$$S_{\eta''\to\eta'} = \frac{I_a}{8\pi c} \frac{(d_{\varepsilon''\Lambda''v''J''} e^{-E_{\varepsilon''\Lambda''v''J''}/kT})}{d_J''\ Q_{tot}} \frac{\omega_{(\varepsilon''\Lambda''v''J'')(\varepsilon'\Lambda'v'J')}}{\omega^3_{(\varepsilon''\Lambda''v'')(\varepsilon'\Lambda'v')}} \tag{11}$$

$$\times (1 - e^{-h\nu_{(\eta''\eta')}/kT}) L_{J''} \frac{d_{\varepsilon'\Lambda'v'}}{d_{\varepsilon''\Lambda''v''}} A_{\varepsilon'\Lambda'v'\to\varepsilon''\Lambda''v''}$$

where the partition function and the energy are no longer approximated and the Hönl–London factor is inserted for the rotational transition-moment squared. Note that the degeneracy factors preceding the Einstein-A coefficient account for the number of J and M states in the upper and lower electronic-vibration states and the degeneracy factors with the partition function term are $d_{\varepsilon\Lambda vJ} = (2S + 1)(2 - \delta_{\Lambda,0})(d_{sym})(2J + 1)$. From the symmetry arguments presented above, it is clear that the ratio of the degeneracy factors, $d_{\varepsilon'\Lambda'v'}/d_{\varepsilon''\Lambda''v''}$, is 2/3 for $X^3\Sigma_g^- \to a^1\Delta_g$ transitions and 1/3 for the $X^3\Sigma_g^- \to b^1\Sigma_g^+$ transitions.

For several of the bands calculated, the program employs the Einstein-A coefficients in units of sec^{-1}. Often one must work from measured vibrational band intensities. In order to make use of these values, we must convert from vibrational band intensity to the Einstein-A coefficient. This relationship was presented in Eq. (10). However, quite often in the literature the vibrational band intensity is reported in units of $cm^{-1}\ km^{-1}\ atm^{-1}$ STP. The values must be converted to the

HITRAN units of $cm^{-1}/(molecule\ cm^{-2})$ to apply the equations presented here. This is accomplished by the relationship

$$S_v^v\left(\frac{cm^{-1}}{molecule\ cm^{-2}}\right) \times \frac{N_L}{p(atm)} \times 10^5 \frac{cm}{km} = S_v^v(cm^{-1}km^{-1}atm^{-1}STP) \tag{12}$$

where N_L is Loschmidt's number, the number of molecules per cubic centimeter of perfect gas at STP. Thus we have

$$S_v^v\left(\frac{cm^{-1}}{molecule\ cm^{-2}}\right) \times 2.6867 \times 10^{24} \frac{cm}{km} = S_v^v(cm^{-1}km^{-1}atm^{-1}STP)\,. \tag{13}$$

From Eq. (10), the Einstein-A coefficients used in the program have been updated using vibrational band intensities reported in the literature. The vibrational band intensities and Einstein-A coefficients used in the program are presented in Table 2 for the $b^1\Sigma_g^+ \leftarrow X^3\Sigma_g^-$ band.

The vibrational band centers are computed using the following expressions

$$G(v) = \omega_e(v + 1/2) - \omega_e x_e(v + 1/2)^2 + \omega_e y_e(v + 1/2)^3 - \omega_e z_e(v + 1/2)^4\,, \tag{14}$$

$$G(v') = \omega_e'(v' + 1/2) - \omega_e x_e'(v' + 1/2)^2 + \omega_e y_e'(v' + 1/2)^3 - \omega_e z_e'(v' + 1/2)^4\,, \tag{15}$$

and

$$\omega_0 = T_e + G(v') - G(v)\,. \tag{16}$$

The constants (T_e, ω_e, $\omega_e x_e$, $\omega_e y_e$, $\omega_e z_e$, ω_e', $\omega_e x_e'$, $\omega_e y_e'$, $\omega_e z_e'$) are taken from Krupenie[16] for both the $a^1\Delta_g^+$ and $b^1\Sigma_g^+$ electronic states.

The partition sums used in the program are those from the TIPS[17] (Total Internal Partition Sum) program. Before addition to the HITRAN database, the line intensities are filtered through a wavenumber dependent cutoff given by

$$S_{cut} = S_{\omega_c}\left(\frac{\omega}{\omega_c}\right)\left\{\frac{1 - e^{-hv/kT}}{1 + e^{-hv/kT}}\right\} \tag{17}$$

with $\omega_c = 2000\ cm^{-1}$ and $S_{\omega_c} = 3.7 \times 10^{-30} cm^{-1}/(molecule\ cm^{-2})$. All lines with an intensity less than the cutoff are not included in the database with the exceptions noted below.

4. HALFWIDTHS

Measurements of the halfwidths are available for several bands of the O_2 molecule. The data of Krupenie[16] are taken for the $X^3\Sigma_g^-$ pure rotation bands, the A-band data are from Ritter and Wilkerson[18], the B-band data from Giver et al[19] and the γ-band data are from Mélières *et al.*[20] The

Table 2. Vibrational band intensities and Einstein-A coefficients for the $b^1\Sigma_g^+ \leftarrow X^3\Sigma_g^-$ band of O_2

Band	S_v^v[a]	S_v^v[b]	A[c]	Ref.	A(ref.)[c]	$A(O_2,CALC)$[c]
A band	532.	1.98×10^{-22}	0.0770	46	0.077	0.077
(0–0)	582.	2.17×10^{-22}	0.084	48	0.084	NA
		2.28×10^{-22}	0.0887	18	0.0887	NA
B band	40.8	1.52×10^{-23}	0.00724	19	NG	0.00591*
(1–0)	38.8	1.44×10^{-23}	0.00689	48	0.0069	NA
γ band	1.52	5.66×10^{-25}	3.2×10^{-4}	47	NG	2.212^{-4}*
(2–0)	1.50	5.58×10^{-25}	3.1×10^{-4}	48	3.2×12^{-4}	NA
	1.26	4.71×10^{-25}	2.6×10^{-4}	20	NG	NA
(3–0)	0.0269	1.00×10^{-26}	6.7×10^{-6}	48	6.7×12^{-6}	NA
(1–1)	0.136	5.06×10^{-26}	0.0701	48	0.0704	0.0704
(0–1)	0.0114	4.24×10^{-27}	0.00467	48	0.0047	0.0047

[a]Units of $cm^{-1}\ km^{-1}\ atm^{-1}$ STP.
[b]Units of $cm^{-1}/(molecule\ cm^{-2})$.
[c]Units of $sec^{-1}/molecule$.
*Does not agree with literature value (see text).
NA not applicable.
NG not given.

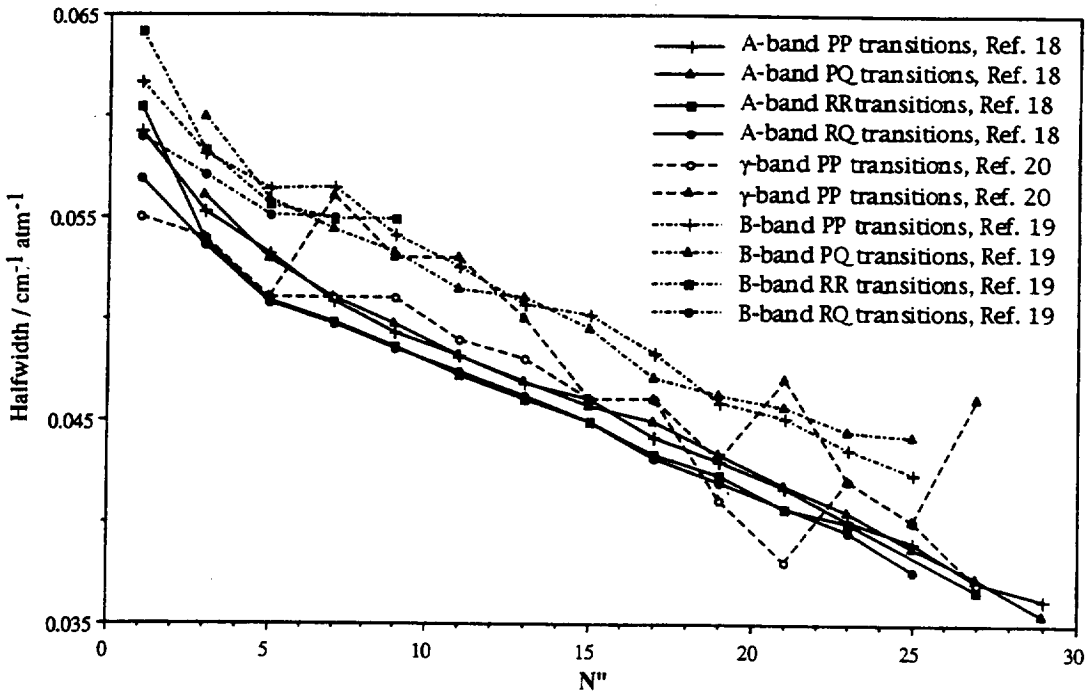

Fig. 2. Halfwidth data cm^{-1} atm^{-1} at 296 K for the *A*-, *B*- and γ bands of O_2 according to branches as a function of *N*.

data of Refs. 18–20 are plotted in Fig. 2 as a function of N'' for the various types of transitions. The transitions are labeled by $\Delta N \Delta J\, N''\, J''$; however with symmetry arguments the notation ${}^{\Delta N}\Delta J_{N''}$ is often used. For the A-band we find that if the ${}^{R}R$ and ${}^{R}Q$ values are shifted, $(N'' \rightarrow N'' + 2)$, they agree with the ${}^{P}P$ and ${}^{P}Q$ values (see Fig. 3), i.e.,

$$\gamma({}^{P}P_{N''}) = \gamma({}^{R}R_{N''+2})$$

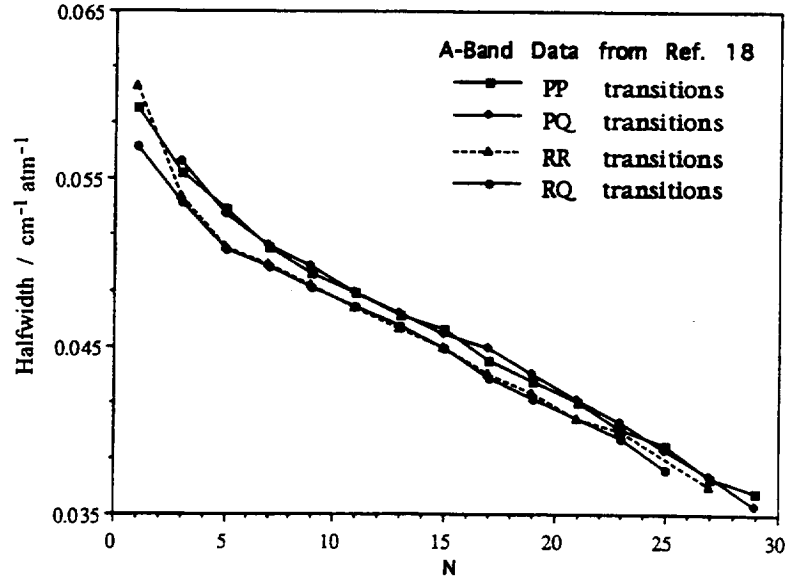

Fig. 3. *A*-band halfwidths cm^{-1} atm^{-1} at 296 K. *RR* and *RQ* values are shifted, $N'' \rightarrow N'' + 2$.

and

$$\gamma(^{P}Q_{N''}) = \gamma(^{R}Q_{N''+2}) \tag{18}$$

For the B-band, the difference between the ^{P}P, ^{P}Q, ^{R}R, and ^{R}Q values for a given N'' is small. The data of Mélières et al[20] for the γ-band, however, show large variations in the halfwidth as a function of N'' not seen in the other data (see open circles and triangles in Fig. 2).

Comparing the values from Refs. 18–20, we find that the A- and γ-band results agree with each other and the B-band results are some 10% larger. The data selected for O_2 on the 1996 HITRAN database use the following procedure for the halfwidths. The $X^3\Sigma_g^-$ pure rotation band uses the data reported by Krupenie[16] for the 60 GHz lines. The electric quadrupole transitions and the transitions involving the $a^1\Delta_g$ state use the A-band values.[18] For the A- and γ-bands, the halfwidths of Ritter and Wilkerson[18] are averaged as a function of N'' for the ^{P}P and ^{P}Q lines together and the ^{R}R and ^{R}Q lines together. We have calculated transitions to $N'' = 80$ and the measurements end at $N'' = 29$; thus it is necessary to extrapolate the data. From the plots, an asymptotic limit of $\gamma = 0.032$ cm^{-1}/atm for $N'' \geq 40$ is estimated. Both the R and P lines use the same asymptotic limit. The values of the halfwidths for the A- and B-bands of O_2 used in the HITRAN96 are given in Table 3.

5. UPDATES TO THE OXYGEN DATA FOR THE 1996 HITRAN DATABASE

Below, the changes made to the data for the 1996 HITRAN database are discussed for each band of molecular oxygen considered. The line position and energy differences are defined as the HITRAN92 value minus the HITRAN96 value. For the line intensities the ratio computed is HITRAN92/HITRAN96. The average and maximum differences were calculated for the line position and energy parameters. For the line intensities, the average, maximum and minimum ratios were calculated.

5.1. The principal isotopic species, $^{16}O_2$

5.1.1. The $X^3\Sigma_g^-$ ($v = 0$)← $X^3\Sigma_g^-$ ($v = 0$) band. The energy levels for the vibrational ground state of the $X^3\Sigma_g^-$ electronic state of $^{16}O_2$ are calculated using the formalism of Rouillé et al.[21] In this work the Hamiltonian included all rotational terms to second order[22] and some terms to third order.[23,24] The molecular constants are those of Rouillé et al.[21] These are compared with the energy values from the previous database (the energy levels for O_2 on the 1982–1992 versions of HITRAN

Table 3. Halfwidths in cm^{-1}/atm for the A- and B-bands of O_2

N''	A – P*	A – R†	B‡	N''	A – P*	A – R†	B‡
1	0.0592	0.0587	0.0616	21	0.0417	0.0406	0.0454
2	0.0574	0.0562	0.0600	22	0.0409	0.0402	0.0447
3	0.0557	0.0538	0.0584	23	0.0402	0.0397	0.0440
4	0.0544	0.0523	0.0571	24	0.0395	0.0386	0.0436
5	0.0531	0.0509	0.0558	25	0.0389	0.0376	0.0432
6	0.0520	0.0503	0.0555	26	0.0380	0.0371	0.0428
7	0.0509	0.0498	0.0552	27	0.0371	0.0366	0.0422
8	0.0502	0.0492	0.0547	28	0.0365	0.0183	0.0418
9	0.0495	0.0486	0.0541	29	0.0358	0.0358	0.0414
10	0.0488	0.0479	0.0531	30*	0.0353	0.0353	0.0410
11	0.0482	0.0473	0.0521	31*	0.0349	0.0349	0.0407
12	0.0475	0.0467	0.0515	32*	0.0345	0.0345	0.0404
13	0.0468	0.0461	0.0509	33*	0.0340	0.0340	0.0400
14	0.0464	0.0455	0.0504	34*	0.0337	0.0337	0.0398
15	0.0459	0.0449	0.0499	35*	0.0334	0.0334	0.0395
16	0.0452	0.0441	0.0488	36*	0.0330	0.0330	0.0394
17	0.0445	0.0432	0.0477	37*	0.0328	0.0328	0.0393
18	0.0438	0.0426	0.0469	38*	0.0324	0.0324	0.0391
19	0.0431	0.0421	0.0461	39*	0.0322	0.0322	0.0390
20	0.0424	0.0413	0.0457	40*	0.0320	0.0320	0.0390

*A-band ^{P}P and ^{P}Q transitions.
†A-band ^{R}R and ^{R}Q transitions.
‡B-band transitions.
*Extrapolated.

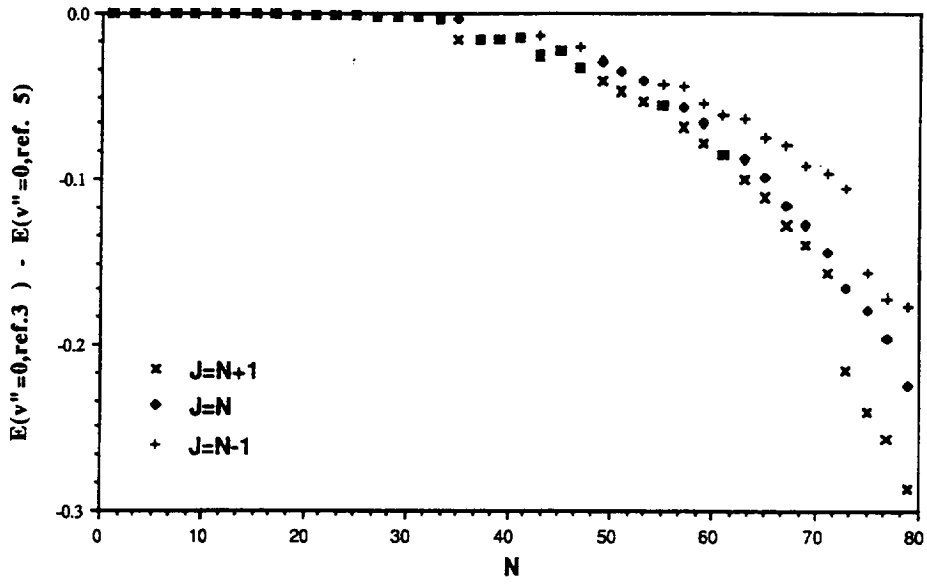

Fig. 4. Energy difference in cm^{-1} between the formalism of Rouillé et al[21] and Greenbaum[13] vs N for the $v'' = 0$ states of $X^3\Sigma_g^-$ of $^{16}O_2$.

used for the formulation of Ref. 13) in Fig. 4. The difference in energy between the two formulations is given as a function of N and J. For the vibrational ground state the difference is near zero for N up to 35, then rapidly goes to $-0.3\ cm^{-1}$ at $N = 80$. While the transition frequencies from this formulation differ only slightly from the previous results, $0.0039\ cm^{-1}$ maximum difference, $7 \times 10^{-5}\ cm^{-1}$ on average, the formalism of Rouillé et al[21] gives better agreement with measurements.‡

This band has both magnetic dipole and electric quadrupole transitions. For the electric quadrupole transitions, a newer value of the quadrupole moment derived from far-IR PIA spectra,[25] 0.34×10^{-26} esu cm^2, has been adopted. There are no data to validate the intensities we obtain. With this value for the quadrupole moment, the line intensities and transition-moments squared are a factor of 5.8 weaker than previous calculations.[26] Because of this reduction in the line intensities, no electric quadrupole lines survived the cutoff for the 1996 data set. This is further discussed below for the 1←0 vibrational band of this electronic band. The 1996 calculations of the magnetic dipole intensities are on average 4% stronger than the 1992 values. This is due to improved energy formulation and partition sums.

5.1.2. The $X^3\Sigma_g^-$ $(v = 1) \leftarrow X^3\Sigma_g^-$ $(v = 0)$ *band.* The 1992 HITRAN database contained only electric quadrupole (eq) lines for this band. The newer data contain both magnetic dipole (md) and electric quadrupole (eq) transitions.[27] Thus, the comparison made here is for the electric quadrupole lines. The energy levels for the vibrational ground ($v = 0$) and the first fundamental ($v = 1$) of the $X^3\Sigma_g^-$ electronic state of $^{16}O_2$ are calculated using the formalism and constants of Rouillé et al.[21] These energies are compared with the values from the previous database[5] in Fig. 5 for the $v'' = 1$ states. The difference is small for N up to ≈ 20 then quickly goes to roughly $5\ cm^{-1}$ at $N = 80$. For the transitions that make the cutoff criterion, $N \leq 31$, the maximum difference in the energy values is $0.0024\ cm^{-1}$, $0.0005\ cm^{-1}$ on average. The corresponding average and maximum differences in the line positions are -0.0104 and $0.0850\ cm^{-1}$. The electric quadrupole transition line intensities are calculated using the formalism of Goldman et al.[27] The absolute intensities are determined by scaling the relative intensities to the measurements of Reid et al.[28] Comparison of these intensities with the 1992 HITRAN values implies an electric quadrupole moment of

‡Comparisons were made with the data from Refs. 20 and 32. The different formulations are compared with experiment for 30 lines measured in Ref. 32 and for 2 transitions measured in Ref. 20. The comparison shows the Rouillé et al formalism to be very slightly better than that of Ref. 13, with the average deviations being $0.00256\ cm^{-1}$ vs. $0.00259\ cm^{-1}$. respectively. Note the average deviation is deceptive in that most of the deviations comes from a few large lines. However on a line-by-line basis the Rouillé et al data are slightly better than the calculations of Ref. 13.

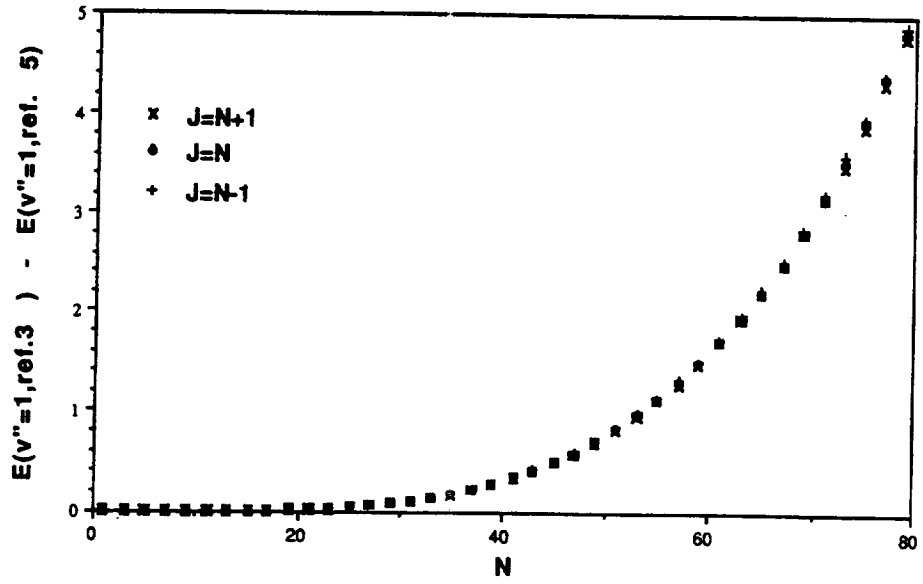

Fig. 5. Energy difference in cm^{-1} between the formalism of Rouillé et al[21] and Greenbaum[13] vs N for the $v'' = 1$ states of $X^3\Sigma_g^-$ of $^{16}O_2$.

0.145×10^{-26} esu cm^2, not in agreement with the quadrupole moment derived from far-I.R. PIA spectra[25] (see previous section). This is under investigation. Comparing the 1996 and 1992 values for the intensities we find an average ratio of 1.0027, with some ratios between 0.740 and 1.31. These large ratios occur for 33 out of the 146 lines and occur only for forbidden (weaker) lines, with $\Delta N \neq \Delta J$ and at low J.

The 1996 calculations for this band are not filtered through a cutoff procedure and many of the lines will have very small intensities. (In fact, one zero intensity magnetic dipole and electric quadrupole transition have been retained in the data for theoretical considerations; it helps to see the effects of assumed parameters on these lines.) There are 254 md transitions and 183 eq transitions retained for this band.

5.1.3. The $X^3\Sigma_g^-$ $(v = 1) \leftarrow X^3\Sigma_g^-$ $(v = 1)$ *band*. As discussed above, the energy differences from the previous calculations and the formulation of Rouillé et al[21] for the $v = 1$ level approach 5 cm^{-1} at N = 80. The maximum energy difference in the lines in the 1996 data is 0.750 cm^{-1} and the average difference is -0.0953 cm^{-1}. The maximum difference in line positions is 0.0457 cm^{-1} with the average difference being -0.00280 cm^{-1}. The intensity ratios are between 0.994 and 0.988 with an average ratio of 0.990. Most of this difference comes from using an improved partition sum in the calculations.

5.1.4. The $a^1\Delta_g$ $(v = 0) \leftarrow X^3\Sigma_g^-$ $(v = 0)$ *band*. There are wavenumber differences which arise from a change in the energy formulation of $X^3\Sigma_g^-$ $(v = 0)$ to that of Rouillé et al[21] and for $a^1\Delta_g$ $(v = 0)$ to that of Scalabrin et al[29] with the constants of Hillig *et al.*[30] The maximum difference is 0.0160 cm^{-1} at $N'' = 37$ and the average difference is -0.00234 cm^{-1}.

The line intensities for this band are calculated using Eq. (11). There are three measurements of the band intensity in the literature (scaled to 296 K) which differ by a factor of about 4.5. The measurement of Badger et al[31] gives $S_{00} = 3.6 \times 10^{-24}$ cm^{-1}/(molecule cm^{-2}). The measurement of Lin et al[32] is $S_{00} = 9.4 \times 10^{-24}$ cm^{-1}/(molecule cm^{-2}), and Hsu et al[33] report a value of $S_{00} = 2.1 \times 10^{-24}$ cm^{-1}/(molecule cm^{-2}). From these values the authors determine the Einstein-A coefficient. Unfortunately, some of the authors have used incorrect statistical degeneracy factors, $d_{g'}/d_u$; Badger et al[31] used 3/2 whereas Lin et al[32] and Hsu et al[33] use 3/1. It was demonstrated above that in Eq. (11) $d_{g'} = 3$ and $d_u = 2$. Thus, application of Eq. (11) (or Eq. (10)) will only generate consistent line intensities if the statistical degeneracy factors and the derived Einstein-A coefficient are from the same author. Because of the large discrepancy between the measured band intensities, we sought to determine the band intensity from another source. We have

Table 4. Measured intensities (Brault and Brown[34]) of the $a^1\Delta_g$ ($v = 0$)← $X^3\Sigma_g^-$ ($v = 0$) band, final HITRAN96 values, ratios, and final average ratio

Line'	Brault and Brown[34] [cm^{-1}/(molecule cm^{-2})]	HITRAN96 [cm^{-1}/(molecule cm^{-2})]	Ratio
O23P22	2.44E-27	2.65E-27	0.92145
O10P18	6.47E-27	6.87E-27	0.94205
P23P23	5.67E-27	5.56E-27	1.019234
P23Q22	6.99E-27	6.12E-27	1.142344
O13P12	1.67E-26	1.62E-26	1.030864
P21P21	9.10E-27	9.36E-27	0.972118
P21Q20	1.02E-26	1.04E-26	0.982659
P19P19	1.43E-26	1.47E-26	0.970808
O11P10	1.90E-26	1.78E-26	1.065022
P19Q18	1.70E-26	1.65E-26	1.030303
P17P17	2.06E-26	2.16E-26	0.954588
O9P8	1.75E-26	1.72E-26	1.018034
P15P15	2.75E-26	2.93E-26	0.937287
P15Q14	3.45E-26	3.38E-26	1.019805
		Average	1.000469

'Branch symbol for ΔN, N''; branch symbol for ΔJ, J''.

obtained unpublished line intensity measurements[34] of 14 transitions in the $a^1\Delta_g$ ($v = 0$)← $X^3\Sigma_g^-$ ($v = 0$) band that were mentioned in the work of Wallace and Livingston.[35] Using our O_2 program, the Einstein-A coefficient used to calculate the line intensities was scaled to match the measurements of Ref. 34. The results are in Table 4. This fit gives a band intensity of $S_{00} = 3.69 \times 10^{-24}$ cm^{-1}/(molecule cm^{-2}) which is close to the Badger et al[31] value. The Einstein-A coefficients, the band intensities, and the statistical degeneracy factors as related by Eq. (10) are listed in Table 5. The calculation of the line intensities for the 1996 database used the Einstein-A coefficient $A = 2.59 \times 10^{-4}$ sec^{-1} with statistical degeneracy factors of $d_l = 3$ and $d_u = 2$. The resulting line intensities are larger than HITRAN92 by roughly a factor of 2; this is due to incorrect inversion from Badger et al's A to S used in previous versions of HITRAN. Suspicion of such missing factors of 2, and concerns about the interpretation of upper atmosphere emissions, such as inferring ozone from SME (Solar Mesophere Explorer via the $a^1\Delta_g$ 1.27 μm airglow) were expressed by Mlynczak and Nesbitt[36] (who conjectured a significant change in A from one of the reported S values in Table 5 (Hsu et al[33])) and by Pendelton et al.[37] Recent observations in the mesosphere[38] confirm the Badger et al[31] value of the Einstein-A coefficient. Moreover, new line intensity measurements made at National Institute for Standards and Technology[39] and at Rutherford Appleton Laboratory[40] are roughly 15% larger than the HITRAN96 values. Preliminary comparisons indicate agreement between these two new independent high-resolution studies. When completed, these data will be incorporated into the next edition of HITRAN.

5.1.5. The $a^1\Delta_g$ ($v = 1$)← $X^3\Sigma_g^-$ ($v = 0$) band. The molecular constants for the $a^1\Delta_g$ ($v = 1$) state are from Brault.[41] Line positions have changed 0.001302 cm^{-1} on average.

The Einstein-A coefficient used is 1/200 of the value of the $a^1\Delta_g$ ($v = 0$)←($v = 0$) band,[42] hence the line intensities are increased by 1.46 on average. Unfortunately, to our knowledge, no other observations of this band are available to perform a proper test of this adopted ratio. The line positions and energies have only changed by -0.000273 cm^{-1} and 0.000388 cm^{-1} on average.

5.1.6. The $a^1\Delta_g$ ($v = 0$)← $X^3\Sigma_g^-$ ($v = 1$) band. The wavenumbers have changed due to the reformulation of the energy expressions for both the upper and lower states,[21,29] resulting in an average change of 0.0157 cm^{-1}. The line intensities are calculated using one tenth of the Einstein-A coefficient of the $a^1\Delta_g$ ($v = 0$)← $X^3\Sigma_g^-$ ($v = 0$) band[42] and are larger than previous HITRAN

Table 5. Measured band intensities, derived Einstein-A coefficients, and statistical degeneracy factors for the $a^1\Delta_g(v = 0)$←$X^3\Sigma_g^-(v = 0)$ band

Reference	S_{00} [cm^{-1}/(molecule cm^{-2})]	$A_{v'v''}$ (sec^{-1})	d_l/d_u
Badger et al[31]	3.66×10^{-24}	2.58×10^{-4}	3/2
Lin et al[32]	9.4×10^{-24}	1.3×10^{-4}	3/1
Hsu et al[33]	2.1×10^{-24}	2.9×10^{-4}	3/1
Fit of data[34]'	3.69×10^{-24}	2.59×10^{-4}	3/2

'Adopted for HITRAN96.

databases[5] by an average of 2.04. The same comment as above applies to the adopted ratio used for this band.

5.1.7. The $b^1\Sigma_g^+$ $(v = 0) \leftarrow X^3\Sigma_g^-$ $(v = 0)$ *band (A-band).* The constants for the $b^1\Sigma_g^+$ $(v = 0)$ state are from Zare et al[43] and those for the $X^3\Sigma_g^-$ $(v = 0)$ state are from Rouillé et al.[21] The wavenumbers differ by $-0.00127\ cm^{-1}$ on average, with the maximum difference being $0.00383\ cm^{-1}$. The average energy difference is $0.00134\ cm^{-1}$. Intensity ratios vary from 0.825 to 0.877, with the average ratio being 0.862. The Einstein-A coefficient has been changed from the value of Miller et al[44] $0.077\ sec^{-1}$ to the newer value of 0.0887 from Ritter and Wilkerson.[18]

5.1.8. The $b^1\Sigma_g^+(v = 1) \leftarrow X^3\Sigma_g^-$ $(v = 0)$ *band (B-band).* The constants for the $X^3\Sigma_g^-$ $(v = 1)$ state are from Zare et al[43] and those for the $X^3\Sigma_g^-$ $(v = 0)$ state are from Rouillé et al.[21] The wavenumber and energies arise from changes made to the ground state energies. The maximum wavenumber and energy differences are $0.00383\ cm^{-1}$ and $0.00370\ cm^{-1}$, respectively. The intensity ratios range from 0.782 to 0.822 with an average of 0.811. The value of the Einstein-A coefficient is from Giver et al,[19] $A(1\text{–}0) = 0.00724\ sec^{-1}$, but was incorrectly used in the previous program where it was set to $A(1\text{–}0) = 0.00591\ sec^{-1}$.

5.1.9. The $b^1\Sigma_g^+$ $(v = 2) \leftarrow X^3\Sigma_g^-$ $(v = 0)$ *band (γ-band).* The constants for the $b^1\Sigma_g^+$ $(v = 2)$ state are also from Zare et al[43] and those for the $X^3\Sigma_g^-$ $(v = 0)$ state are from Rouillé et al.[21] The average wavenumber and energy differences are $0.00694\ cm^{-1}$ and $0.00104\ cm^{-1}$. The intensity ratios range from 1.22 to 1.27. The Einstein-A coefficient of Mélières et al[20] is now used, $A(2\text{–}0) = 2.69 \times 10^{-4}\ sec^{-1}$. Compared with the older value from Miller et al[45] of $A(2\text{–}0) = 3.24 \times 10^{-4}\ sec^{-1}$ (which was incorrectly used as $A(2\text{–}0) = 2.2 \times 10^{-4}\ sec^{-1}$ in the HITRAN82[5] calculations) an average ratio of 0.813 is obtained.

5.1.10. The $b^1\Sigma_g^+$ $(v = 1) \leftarrow X^3\Sigma_g^-$ $(v = 1)$ *band.* The molecular constants used in the calculation of energies are from Zare et al[43] for the $b^1\Sigma_g^+$ $(v = 1)$ state and from Rouillé et al[21] for the $X^3\Sigma_g^-$ $(v = 1)$ state. The line positions show a maximum difference of $0.0857\ cm^{-1}$ with an average of $0.0207\ cm^{-1}$. The difference is due to the change in the ground state energies. The Einstein-A coefficient is from Giver *et al.*[19] The intensity ratios range from 0.962 to 0.999. These changes are due to the correct partition sums and removal of some approximations in the formulas.

5.1.11. The $b^1\Sigma_g^+$ $(v = 0) \leftarrow X^3\Sigma_g^-$ $(v = 1)$ *band.* The molecular constants are from Zare et al[43] for the $b^1\Sigma_g^+$ $(v = 0)$ state and from Rouillé et al[21] for the $X^3\Sigma_g^-$ $(v = 1)$ state. The changes in the line positions are from the new lower state energies. The maximum value is $0.0333\ cm^{-1}$ and the average is $0.00935\ cm^{-1}$. The Einstein-A coefficient is from Galkin.[46] The resulting intensity ratios range from 0.968 to 1.00.

5.2. The $^{16}O^{18}O$ species

5.2.1. The $X^3\Sigma_g^-$ $(v = 0) \leftarrow X^3\Sigma_g^-$ $(v = 0)$ *band.* The present calculations use the improved molecular constants of Mizushima and Yamamoto.[47] The resulting energies differ from previous calculations by $0.0174\ cm^{-1}$ on average with a maximum difference of $0.136\ cm^{-1}$ at $N = 53$. The average difference in line position is $0.00112\ cm^{-1}$ with the largest difference being $0.00962\ cm^{-1}$. The line intensities differ only by a few percent maximum which is attributed to the improved partition sums.

5.2.2. The $a^1\Delta_g$ $(v = 0) \leftarrow X^3\Sigma_g^-$ $(v = 0)$ *band.* There is a slight change in some of the wavenumbers due to the change in energy formulation for the $X^3\Sigma_g^-$ $(v = 0)$ state [21]. This gives rise to a maximum difference of $0.00580\ cm^{-1}$ and an average difference of $-0.00127\ cm^{-1}$. Intensity ratios are ≈ 0.5 as expected and 49 of the previous lines do not make the intensity cut off.

5.2.3. The $b^1\Sigma_g^+$ $(v = 0) \leftarrow X^3\Sigma_g^-$ $(v = 0)$ *band.* The energies of the $X^3\Sigma_g^-$ $(v = 0)$ state are calculated using the constants of Mizushima and Yamamoto.[47] The constants for the $b^1\Sigma_g^+$ $(v = 0)$ state are from Babcock and Herzberg.[48] Wavenumber differences of $0.0242\ cm^{-1}$ at $N'' = 34$ are observed with an average difference of $-0.00577\ cm^{-1}$. The average intensity ratio is 0.882 due mostly to the change in partition functions.

5.2.4. The $b^1\Sigma_g^+$ $(v = 1) \leftarrow X^3\Sigma_g^-$ $(v = 0)$ *band.* The constants for the $b^1\Sigma_g^+$ $(v = 1)$ state are from Benedict.[49] Those for the $X^3\Sigma_g^-$ $(v = 0)$ state are from Mizushima and Yamamoto.[47] The maximum wavenumber difference is $0.0107\ cm^{-1}$. This difference is due to the change in the lower state energies. The Einstein-A coefficient is from Giver et al.[19] The average ratio of the intensities 0.830.

5.2.5. The $b^1\Sigma_g^+$ $(v = 2) \leftarrow X^3\Sigma_g^-$ $(v = 0)$ *band.* The constants for the $b^1\Sigma_g^+$ $(v = 2)$ state are from Zare *et al.*[43] Those for the $X^3\Sigma_g^-$ $(v = 0)$ state are from Mizushima and Yamamoto.[47] The maximum wavenumber difference is 0.150 cm^{-1} and the average intensity ratio is 0.837. Caution must be used in interpreting these numbers since the comparison is based on only 3 lines.

5.3. The $^{16}O^{17}O$ *species*

5.3.1. The $X^3\Sigma_g^-$ $(v = 0) \leftarrow X^3\Sigma_g^-$ $(v = 0)$ *band.* The data for this band are taken from the Jet Propulsion Laboratory catalogue.[50] There are 10 787 lines in the JPL file. The data were filtered through the wavenumber dependent cutoff resulting in 2601 lines from 0.000012 cm^{-1} to 186.15 cm^{-1} in the final file. Note the isotopic abundance factor was inadvertently omitted from the 1996 HITRAN database. Thus, the ratio of the line intensity (S92/S96) is 0.000750 on average. In order to properly use the intensities for these data, they should be multiplied by $I_a = 0.000742235$. The line positions and lower state energies have only changed slightly, 0.000041 cm^{-1} and -0.000352 cm^{-1} average difference respectively.

5.3.2. The $b^1\Sigma_g^+$ $(v = 1) \leftarrow X^3\Sigma_g^-$ $(v = 0)$ *band.* These data are from Benedict and Brault[51] and have not changed from the 1982 HITRAN database.

6. OTHER CHANGES

We have added reference and error codes to the line parameter database. The error code (see HITRAN96 manual[52]) for the halfwidths is set to 4. The error code for the line positions of $X^3\Sigma_g^- \leftarrow X^3\Sigma_g^-$ electronic band is set to 4 and all other error codes are not utilized on the database (i.e. set to 0). We have also labeled the electric quadrupole and magnetic dipole transitions by the lower case letters *q* and *d*, respectively, in the sym field of the rotational quantum number character string, i.e., Br, F'',__;Br, N'', Br, J'', ____, Sym.

These data are available in the 1996 HITRAN database.[52]

7. O_2 CONTINUUM ABSORPTION

It is known that the $O_2 X^3\Sigma_g^-(v'') - a^1\Delta_g(v')$ absorption bands exhibit both discrete (rotational) line structure and pressure-induced continuous absorption.[31] The most important bands are the $v'' = 0$, $v' = 0$ at 1.27 μm (7882 cm^{-1}), $v'' = 0$, $v' = 1$ at 1.06 μm (9366 cm^{-1}), and $v'' = 1$, $v' = 0$ at 1.6 μm (6326 cm^{-1}). While the rotational lines of the (0–1) band are weaker than those of (0–0) band, and those of (1–0) band are weaker than the (0–1) band, the continuum absorptions are of more similar intensity.

During the update of the (0–0) band line parameters, theoretical calculations were compared with absolute atmospheric transmittance obtained with the University of Denver Absolute Solar Transmittance Interferometer (ASTI).[53] The results show good agreement of the line structure but a clear indication of the underlying continuum (not modeled), with the *P*, *R* (no *Q*) shape of the envelope under the absorption lines. The continuum is clearer at the higher spectral resolution (≥ 0.5 cm OPD).

More recent ASTI data in the 9400 cm^{-1} and 6400 cm^{-1} regions also show a strong continuum, similar to that described above. It is thus proposed that this is due to the pressure-induced absorption of the $v'' = 0$, $v' = 1$ and $v'' = 1$, $v' = 0$ bands respectively.[54] Laboratory data[55] are consistent with these conclusions, but indicate no pressure-induced absorptions under the $X^3\Sigma_g^-(v'') - b^1\Sigma_g^+(v')$ bands. The pressure-induced absorption in the $X^3\Sigma_g^-(v'' = 0) - X^3\Sigma_g^-(v' = 1)$ has been well documented in previous publications.[25, 56, 57]

In the HITRAN database we have included the individual line parameters of these bands, but no cross-sections are provided for the continuum. These cross-sections will be forthcoming on the next version of the HITRAN database.

Acknowledgements—The authors are pleased to acknowledge support of this research by the Air Force Office of Scientific Research Task 2310G1. The research at the University of Denver was also supported by the National Science Foundation, Atmospheric Chemistry Division.

REFERENCES

1. Thomas, R. J., Barth, C. B., Rusch, D. W. and Sanders, R. W., *J. Geophys. Res.*, 1984, **89**, 9569.
2. Mlynczak, M. G., Solomon, S. and Zarus, D. S., *J. Geophys. Res.*, 1993, **98**, 18,639.
3. Rothman, L. S. and Goldman, A., *Appl. Opt.*, 1981, **20**, 2182.
4. Rothman, L. S., Gamache, R. R., Goldman, A., Flaud, J.-M., Tipping, R. H., Rinsland, C. P., Smith, M. A. H., Toth, R. A., Brown, L. R., Devi, V. M. and Benner, D. C., *J. Quant. Spectrosc. Radiat. Transfer*, 1992, **48**, 469.
5. Rothman, L. S., Gamache, R. R., Barbe, A., Goldman, A., Gillis, J. R., Brown, L. R., Toth, R. A., Flaud, J.-M. and Camy-Peyret, C., *Appl. Opt.*, 1983, **22**, 2247.
6. Cohen, E. R. and Taylor, B. N., *Phys. Today*, 1995, August, BG9–BG13.
7. Herzberg, G., *Molecular Spectra and Molecular Structure I. Spectra of Diatomic Molecules*, 2nd edn. Van Nostrand, New York, 1966.
8. Herzberg, G., *Molecular Spectra and Molecular Structure II. Infrared and Raman Spectra of Polyatomic Molecules*. Van Nostrand, New York, 1960.
9. Tinkham, M. and Strandberg, M. W. P., *Phys. Rev.*, 1955, **97**, 937.
10. Steinbach, W. and Gordy, W., *Phys. Rev. A*, 1973, **8**, 1753.
11. Steinbach, W. and Gordy, W., *Phys. Rev. A*, 1975, **11**, 729.
12. Steinbach, W. R., Millimeter and submillimeter wave spectra of the oxygen isotopes: $^{16}O_2$, $^{18}O_2$, and $^{16}O^{18}O$. Ph.D. Thesis, Department of Physics, Duke University, 1974.
13. Greenbaum, M., The calculation of millimeter and submillimeter wave absorption line parameters for the molecular oxygen isotopes: $^{16}O_2$, $^{16}O^{18}O$, $^{18}O_2$. Riverside Research Institute Technical Report T-1/306-3-14,80, West End Avenue, New York, NY 10023, 1975.
14. Penner, S. S., *Quantitative Molecular Spectroscopy and Gas Emissivities*. Addison-Wesley, Reading, MA, 1959.
15. Gamache, R. R. and Rothman, L. S., *J. Quant. Spectrosc. Radiat. Transfer*, 1992, **48**, 519.
16. Krupenie, P. H., *J. Phys. Chem. Ref. Data*, 1972, **2**, 423.
17. Gamache, R. R., Hawkins, R. L. and Rothman L. S., *J. Mol. Spectrosc.*, 1990, **142**, 205.
18. Ritter, K. J. and Wilkerson, T. D., *J. Mol. Spectrosc.*, 1987, **121**, 1.
19. Giver, L. P., Boese, R. W. and Miller, J. H., *J. Quant. Spectrosc. Radiat. Transfer*, 1974, **14**, 793.
20. Mélières, M. A., Chenevier, M. and Stoeckel, F., *J. Quant. Spectrosc. Radiat. Transfer*, 1985, **33**, 337.
21. Rouillé, G., Millot, G., Saint-Loup, R. and Berger, H., *J. Mol. Spectrosc.*, 1992, **154**, 372.
22. Loete, M. and Berger, H., *J. Mol. Spectrosc.*, 1977, **68**, 317.
23. Welch, W. M. and Mizushima, M., *Phys. Rev. A*, 1972, **5**, 2692.
24. Zink, L. R. and Mizushima, M., *J. Mol. Spectrosc.*, 1987, **125**, 154.
25. Cohen, E. R. and Birnbaum, G., *J. Chem. Phys.*, 1977, **66**, 2443.
26. Benedict, W. S. and Kaplan, L. D., *J. Quant. Spectrosc. Radiat. Transfer*, 1964, **4**, 453.
27. Goldman, A., Rinsland, C. P., Canova, B., Zander, R. and Dang-Nhu, M., *J. Quant. Spectrosc. Radiat. Transfer*, 1995, **54**, 757.
28. Reid, J., Sinclair, R. L., Robinson, A. M. and McKellar, A. R. W., *Phys. Rev. A*, 1981, **24**, 1944.
29. Scalabrin, T., Saykally, R. J., Evenson, K. M., Radford, H. E. and Mizushima, M., *J. Mol. Spectrosc.*, 1981, **89**, 344.
30. Hillig II, K. W., Chiu, C. C. W., Read, W. G. and Cohen, E. A., *J. Mol. Spectrosc.*, 1985, **109**, 205.
31. Badger, R. M., Wright, A. C. and Whitlock, R. F., *J. Chem. Phys.*, 1965, **43**, 4345.
32. Lin, L.-B., Lee, Y.-P. and Ogilvie, J. F., *J. Quant. Spectrosc. Radiat. Transfer*, 1988, **39**, 375.
33. Hsu, Y. T., Lee, Y. P. and Ogilvie, J. F., *J. Quant. Spectrosc. Radiat. Transfer*, 1992, **48A**, 1227.
34. Brault, J. and Brown, M. M., Unpublished results.
35. Wallace, L. and Livingston, W., *J. Geophys. Res.*, 1990, **95**, 9823.
36. Mlynczak, M. G. and Nesbitt, D. J., *Geophys. Res. Lett.*, 1995, **22**, 1381.
37. Pendelton, W. R. jr, Baker, D. J., Reese, R. J. and O'Neil, R. R., *Geophys. Res. Lett.*, 1996, **23**, 1013.
38. Sandor, B. J., Clancy, R. T., Rusch, D. W., Randall, C. E., Eckman, R. S., Siskind, D. S. and Muhleman, D. O., *J. Geophys. Res.*, 1997, **102**, 9013.
39. Lafferty, W., National Institute of Standards and Technology, Private communication, 1996.
40. Newnham, D. A., Ballard, J. and Page, M. S., Visible absorption spectroscopy of molecular oxygen, Paper A7, Atmospheric Spectroscopy Applications Workshop, 4–6 September 1996. Reims, France.
41. Brault, J., Private communication, 1982.
42. Jones, A. V. and Harrison, A. H., *J. Atmos. Terr. Phys.*, 1958, **13**, 45.
43. Zare, R. N., Schmeltekopf, A. L., Harrop, W. J. and Albritton, D. L., *J. Mol. Spectrosc.*, 1973, **46**, 37.
44. Miller, J. H., Boese, R. W. and Giver, L. P., *J. Quant. Spectrosc. Radiat. Transfer*, 1969, **9**, 1507.
45. Miller, J. H., Giver, L. P. and Boese, R. W., *J. Quant. Spectrosc. Radiat. Transfer*, 1976, **16**, 595.
46. Galkin, V. D., *Opt. Spectrosc. (USSR)*, 1979, **47**, 151.
47. Mizushima, M. and Yamamoto, S., *J. Mol. Spectrosc.*, 1991, **148**, 447.
48. Babcock, H. and Herzberg, L., *Astrophys. J.*, 1948, **108**, 167.
49. Benedict, W. S., Private communication, 1982.
50. Poynter, R. L., Pickett, H. M., Cohen, E. A., Delitsky, M. L., Pearson, J. C. and Müller, H. S. P.,

Submillimeter, millimeter, and microwave spectral line catalogue, JPL publication 80-23, Revision 4, 10 March 1996.
51. Benedict, W. S. and Brault, J., Private communication, 1982.
52. Rothman, L. S., Rinsland, C. P., Goldman, A., Massie, S. T., Edwards. D. P., Flaud, J.-M., Perrin, A., Dana, V., Mandin, J.-Y., Schroeder, J., McCann, A., Gamache, R. R., Wattson, R. B., Yoshino, K., Chance, K. V., Jucks, K. W., Brown L. R., Nemtchinov, V., and Varanasi P., in preparation.
53. Goldman, A., The role of laboratory spectroscopy in the analysis of atmospheric spectra, Atmospheric Spectroscopy Applications (ASA) Colloquium, Reims, France, 4–6 September 1996.
54. Goldman, A., Extended quantitative spectroscopy for analysis of atmospheric infrared spectra, Fourier Transform Spectroscopy OSA—Topical Meeting, Santa Fe, New Mexico, 10–12 February 1997.
55. Greenblat, G. D., Orlando, J. J., Burkholder, J. B. and Ravishankara, A. R., *J. Geophys. Res.*, 1990, **95**, 18,577.
56. Orlando, J. J., Tyndall, G. S., Nickerson, K. E. and Calvert, J. G., *J. Geophys. Res.*, 1991, **96**, 20,755.
57. Rinsland, C. P., Smith, M. A. H., Seals, R. K. jr, Goldman, A., Murcray, F. J., Murcray, D. G., Larsen, J. C. and Rarig, P. L., *J. Geophys. Res.*, 1982, **87**, 3119.